The Dynamic Effects of Weather Shocks on Agricultural Production

Cédric Crofils[✉a,b], Ewen Gallic[b], and Gauthier Vermandel[c,d,a]

[a]LEDa, Paris-Dauphine & PSL Universities
[b]Aix Marseille Univ, CNRS, AMSE, Marseille, France.
[c]CMAP, Ecole polytechnique, Institut Polytechnique de Paris
[d]Banque de France, 31 rue Croix des Petits Champs, 75049 Paris, France.

November, 2024

Journal of Environmental Economics and Management, 130, 103078.
doi: 10.1016/j.jeem.2024.103078

Abstract

This paper proposes a new methodological approach using high-frequency data and local projections to assess the impact of weather on agricultural production. Local projections capture both immediate and delayed effects across crop types and growth stages, while providing early warnings for food shortages. Adverse weather shocks, such as excess heat or rain, consistently lead to delayed downturns in production, with heterogeneous effects across time, crops, and seasons. We build a new index of aggregate weather shocks that accounts for the typical delay between event occurrence and economic recognition, finding that these shocks are recessionary at the macroeconomic level, reducing inflation, production, exports and exchange rates.

JEL classification Numbers: C23, E32, Q11, and Q54

Keywords: Weather shocks, Agriculture, Local projections, VAR

We thank Olivier Deschenes, Garance Genicot, Loïc Henry, Elise Huillery, Aymeric Ortmans, Evi Pappa, Juan-Pablo Rud and Emilien Veron for their remarks, as well as seminar participants at University College London, Université Paris-Dauphine. We also thank the contributors at the conferences where this research was presented: the EEA Congress 2023, the EAERE 28th Annual Conference, the 63rd Annual Meeting of the Société Canadienne de Science Économique, the 29th CEF International Conference, the AFSE 2023 Annual Congress, the 22nd Journées LAGV, the 20th Augustin Cournot Doctoral Days, the 12th EconomiX PhD Student Conference, the Dauphine Economics Doctoral Day, the 95th International Atlantic Economic Conference, Banque de France Clifirium conference, and Stress-test seminar of Institut Polytechnique for their valuable and insightful feedback. The authors also thank the Editor Klaus Moeltner and two anonymous referees.
Cedric Crofils acknowledges funding from the Collectivité Territoriale de Martinique. Ewen Gallic acknowledges that the project leading to this publication has received funding from the French government under the "France 2030" investment plan managed by the French National Research Agency (reference: ANR-17-EURE-0020) and from the Excellence Initiative of Aix-Marseille University—A*MIDEX. Gauthier Vermandel acknowledges funding from the chair Stress-test hosted by Institut Polytechnique de Paris.

✉Corresponding author: cedric.crofils@dauphine.psl.eu. University Paris Dauphine – PSL Research University, LEDa UMR CNRS 8007, Place du Maréchal de Lattre de Tassigny, 75775 Paris Cedex 16, France.

1 Introduction

Weather shocks, or abnormal weather events, can have serious economic consequences, particularly for vulnerable sectors like agriculture. Given these vulnerabilities, the objective of this study is to quantitatively measure the dynamic effects of abnormal weather on the supply of agricultural products over time. Assessing the consequences of an unexpected weather event observed today on future crop production is essential for anticipating adverse outcomes. This is particularly crucial in the context of climate change, where certain countries, especially in the tropics, face significant increases in temperature and precipitation variability (Castellanos et al., 2022). At the farmer level, such a quantitative analysis can aid in making better-informed decisions to adapt to climate change. At the macroeconomic level, these assessments are important for policymakers to anticipate potential food shortages and income losses, enabling them to implement effective mitigation policies.

Our empirical approach examines the impact of weather fluctuations on agricultural production in Peru, using monthly regional and crop-specific data. The analysis employs a linear panel model with local projections to leverage exogenous within-regional variations in weather fluctuations to assess how random changes in the weather affect agricultural production across months, regions, and crops. Our measures of weather shocks are based on precipitation and temperature. We extract the unexpected component of the weather by taking the deviation of the weather variable from its historical average.[1]

The literature examining how the weather affects agricultural production typically bases its quantitative analysis on annual data (see, *e.g.*, Deschênes and Greenstone, 2007; D'Agostino and Schlenker, 2016; Burke and Emerick, 2016; Jagnani et al., 2021). The standard approach in the field to measuring the effects of the weather on economic outcome is through the panel fixed effects framework. Studies with panel fixed effects typically use weather data frequencies ranging from annual to daily, with annual economic data being most common.[2] This methodology has been extensively applied in the literature, including the analysis of weather impacts on agriculture and broader economic indicators.

With respect to the baseline panel fixed effects framework, we propose a complementary methodological approach that comprises two core ingredients: high-frequency agricul-

[1] We compute the average monthly maximum regional extreme daytime temperature and total rainfall and express each as a weather anomaly by taking the deviation of the weather variable from its historical average. Intergovernmental Panel on Climate Change (IPCC) studies, such as Parry et al. (2007), have documented a large negative sensitivity of crop production to extreme daytime temperatures and precipitation. We build on this observation to construct the weather variables.

[2] Most studies using the panel fixed effects framework focus on crops with highly seasonal production, such as corn and soybeans in the U.S. context, while this paper investigates tropical agriculture, where some crops are produced year-round. This introduces a different dynamic, as tropical crops face continuous exposure to weather shocks throughout the year.

tural production data combined with local projections (LPs).[3] The panel fixed effects standard in agricultural economics typically maps current economic variables (y_t) to current and past weather variables ($w_t, w_{t-1}, \ldots$) through a function f: $y_t = f(w_t, w_{t-1}, \ldots)$. Local projections, on the other hand, reverse this approach by forecasting the response of an economic variable over multiple horizons (h) conditional on a weather shock, $y_{t+h} = f(w_t, w_{t-1}, ...)$ with $h = 0, 1, \ldots$, thereby providing a dynamic view of the impact over time. We exploit the plausibly exogenous variations in temperature and precipitation at the Peruvian regional level to study the delayed effects of weather shocks on agricultural production over multiple months after the realization of the shock. We control for regional fixed effects, dynamic macroeconomic characteristics, and temporal dependence. By leveraging the cross-sectional dimension at the regional level, we use impulse response analysis to identify the propagation of a regional weather shock on agricultural production. Why are local projections particularly well-suited for measuring the effects of weather shocks on intra-annual data? The biological growing process of crops introduces a natural time lag between the month of the realization of a weather shock and the month of its economic impact at harvest time. Impulse response functions directly coincide with the life-cycle of a weather shock from its realization up to its disappearance in economic terms.

Our methodology, based on LP in high frequency, provides four main additional advantages with respect to the current panel fixed effects standard in agricultural economics. First, this methodology provides a straightforward mapping of economic costs with random weather variations, avoiding possible ambiguities present in aggregate annual data. These ambiguities may concern both agricultural,[4] and weather data.[5] Aggregation can affect the estimated impacts of weather shocks; we find that the impact of a shock is smaller when using aggregate data.

A second advantage of high-frequency local projections is their ability to assess the time-varying vulnerability of crops across different growth stages, as crops are generally more vulnerable during the early stages of growth than at the harvesting stage. To capture these

[3] Local projections pioneered by Jordà (2005) are an econometric framework that has become widely used for measuring impulse response functions in various fields of applied economics. LPs are not only relatively more robust to misspecification but are also easy to estimate (via linear regression) and accommodate in panel data.

[4] If the harvesting season spans two calendar years, it could potentially complicate the mapping of weather events to their true realization, depending on how the statistical service conducts surveys or data gathering. In some cases, data may be collected based on the crop year rather than the calendar year, which would mitigate this issue. However, in Peru, where the harvesting peak for maize, for example, occurs in December, the production from one growing season spreads across two calendar years. This makes it more challenging to align economic impacts with weather events. Additionally, in tropical agriculture, where crops can be produced year-round, defining distinct growing seasons is often more complex.

[5] The annualization of weather data can also omit relevant information regarding the effects of weather on agriculture (Cui et al., 2024). Specifically, the mean-wise aggregation of extreme weather events throughout the year can average out the impact of both positive and negative events (Colacito et al., 2019), potentially underestimating the true damages caused by weather shocks on agriculture. A typical approach to address this aggregation masking effect is to consider sub-annual (*e.g.*, season-dependent anomalies) and non-linear (*e.g.*, temperature bins or degree-days) weather metrics.

heterogeneous effects of weather shocks over time, the literature employs various techniques to disaggregate weather metrics. Some studies distinguish between different seasons (*e.g.*, Tack et al., 2017; Schmitt et al., 2022), growing seasons (*e.g.*, Ortiz-Bobea and Just, 2012; Chen et al., 2016; D'Agostino and Schlenker, 2016; Gammans et al., 2017; Taraz, 2018; Jagnani et al., 2021), or fine stages of the growth process such as vegetative, ripening, and maturation phases (*e.g.*, Ortiz-Bobea et al., 2019; Welch et al., 2010). Other approaches use more granular metrics, such as monthly data (*e.g.*, Miao et al., 2016; Yu and Goh, 2019; Li, 2023) or weekly observations (*e.g.*, Powell and Reinhard, 2016).[6] In most of these studies, the variable of interest often remains annual, which does not allow for the identification of the intra-year dynamics of shocks within the season. In contrast, local projections at a monthly frequency naturally capture the time-varying vulnerability of crops across different growth stages: impulse response functions (IRFs) at shorter horizons isolate the effects on crops that are already mature, while IRFs at longer horizons capture the delayed effects on crops that were affected in their early stages of growth. By comparing the size of the IRF at different horizons, one can directly measure the heterogeneous effects of weather shocks across the growing to harvesting stages and identify when crops are most vulnerable.

A third advantage of our methodology, related to the horizon of the IRF, is the ability to identify permanent effect of weather shocks. By leveraging the granularity of our monthly data, one can compute the average duration in months of a crop cycle from planting to harvesting. Hysteresis is identified from any impulse response function that persists beyond the typical crop cycle duration.

A last advantage of high-frequency LPs on agricultural production is their capacity to provide early warnings for policymakers to anticipate food security. By collecting and monitoring daily weather data, policymakers can predict regional food shortages several months in advance when an abnormally large weather shock occurs.

While our analytical framework offers distinct advantages, it also presents limitations compared to more widely used methods in the literature. The use of monthly production data, as opposed to annual data, emphasizes the short-term effects of weather fluctuations. This higher frequency of data complicates the identification of long-term effects. Although our framework can highlight certain adaptation mechanisms, longer-term changes are better captured using the traditional methods in the literature that rely on annual data.

From our empirical analysis, we derive three main findings. First, while it is well-known that weather shocks are overall detrimental to agriculture, we corroborate this finding by distinguishing heterogeneous effects on agricultural production. This heterogeneity depends

[6] Interestingly, the Peruvian context differs from previous studies. In addition to the crops typically studied in the USA (such as maize), our database includes tropical crops such as cassava. The longer and more spread-out growing process of the crops makes the use of conventional tools (ie. distinction between growing periods) more complicated, while local projections remain suitable.

on the type of crop, the type of weather shock, and the season (growing season versus harvesting season). Specifically, a weather shock, defined here as an abnormally high monthly realization compared to the regional average, can cause a significant 5% to 15% monthly decline in agricultural production for any crop type in our sample, with temperature shocks being more detrimental than precipitation shocks. Weather shocks during the growing season have a more substantial impact than those occurring during the harvest season, indicating the critical timing of these events.

Our second key finding reveals the presence of hysteresis effects from weather shocks, which can be attributed to several factors. These include lost income, loss of inputs (*e.g.*, seeds), delays in reallocating land or other resources, and changes in the composition of farmers in a given region. One possible explanation is a learning mechanism, where farmers adjust their crop mix in subsequent growing seasons. This decline may reflect a strategic response, with farmers choosing not to plant the same crops in consecutive seasons, resulting in scarring effects from weather shocks.[7]

Finally, our third main takeaway addresses the aggregate implications of weather shocks. Instead of focusing on the channel of impact directly on aggregate outcomes, as in the literature,[8] we aggregate in-sample responses of regional crop production to weather shocks from LPs and net the contributions of all current and past weather shocks on current agricultural production to develop a national macroeconomic index of weather shock losses. When fed into a Vector Autoregression (VAR) model alongside other core macro variables, we find that a representative weather shock leads to a 0.4% decline in agricultural production, a 1.5% decline in exports, an immediate decline in the real domestic currency, and a modest reduction in inflation. These results highlight that the implications are not only local but can also cause fluctuations at the country level that can affect the conduct of stabilization policies. In particular, the VAR predicts that monetary policy reduces interest rate in response to a weather shock to revive the economy.

Our study is connected to two complementary branches of literature. The first strand of the literature examines the nexus between economic growth and climate based on yearly data. Dell et al. (2012) demonstrate that higher temperatures reduce economic growth and agricultural production in a large panel of countries. Building on this study, the research question has been extended in several directions.[9] Colacito et al. (2019) conduct a similar exercise for the US economy and find that rising summer temperatures have a pervasive effect

[7] Note that this article does not aim to directly address the adaptation strategies implemented by farmers in response to weather fluctuations, as explored by Sesmero et al. (2018); Jagnani et al. (2021); Blakeslee et al. (2020) or Bareille and Chakir (2024), among others. However, our findings suggest that production can remain affected even after harvest, implicitly indicating some degree of farmer adaptation.

[8] See, for example, Acevedo et al. (2020), who identify negative impacts of weather shocks on agricultural and aggregate output in developing countries.

[9] While most of the literature examines the effects of weather variables on quantities, Faccia et al. (2021) explore the effects on prices and identify deflationary effects.

on the entire cross-section of industries. Ortiz-Bobea et al. (2021) employ a country-level panel regression and yearly data from 1961 to 2015 to investigate the impact of climate change on agricultural Total Factor Productivity (TFP). The authors conclude that, on average, in Latin America, climate change had a negative impact on agricultural TFP, reducing it by more than 25% over the sample period, attributable to variations in average temperature and total rainfall.

The second strand of literature focuses on estimating the effects of weather and climate change on agriculture, employing agronomic models and statistical models (see D'Agostino and Schlenker 2016 for a review). The latter, which is predominant in the economic literature, has shifted from cross-sectional (Mendelsohn et al., 1994) to panel data analysis (see Blanc and Schlenker 2017, or Kolstad and Moore 2020). These models, which assess variables, such as crop yield (Schlenker and Roberts 2009), production (Lesk et al. 2016), and profit (Deschênes and Greenstone 2007) over space and time, account for both group- and time-specific effects. The former captures constants such as soil quality, while the latter considers factors affecting all regions in a given year. Panel regressions, treating weather variations as exogenous, offer insights into short-term effects, although caution is needed in long-term studies, as rapid farmer adaptation can skew the results (Kolstad and Moore, 2020).[10] Our study relies on panel data such as this second strand of literature, and focuses on short-term effects. However, we adopt a distinct framework that not only links year-to-year variations in agricultural production with changing weather conditions but also facilitates the exploration of dynamic propagation effects.

The remainder of this article is organized as follows. Section 2 describes the data and the variables used in the empirical analysis. Section 3 details the estimation strategy and discusses the panel estimation results. Section 4 examines the differentiated effects of weather shocks across production stages, distinguishing between a growth regime and a harvest regime. Section 5 shifts the focus from agricultural production and investigates the transmission of weather shocks to the rest of the nation's economy. Section 6 provides a conclusion.

2 Data

This section presents the data, outlines the transformations applied for quantitative analysis, and provides descriptive statistics for the agricultural data.

2.1 Data Sources and Transformations

Regional Agricultural Data. Our primary source of agricultural data is derived from monthly agricultural reports, *El Agro en Cifras*, produced by the Ministry of Agriculture and

[10] To study long-term effects, Burke and Emerick (2016) suggest a framework in which they model the change in average yields at two different points in time for a given location as a function of changes in average temperature.

Irrigation of Peru (MINAGRI) spanning from 2001 to 2019. We extracted data on production (measured in tons) and on the planted and harvested areas (measured in hectares) for each of the primary crops cultivated in Peru across 25 administrative regions, covering the period from January 2001 to December 2015. Four main crops are analyzed in this study: potato (*papa*), cassava (*yuca*), rice (*arroz cáscara*), and maize (*maíz amarillo duro*). The selected crops in this study collectively represent a substantial share of agricultural production, comprising 53% of the cultivated surface and 37% of the total production in Peru. To deal with seasonality, we express agricultural production as its normalized value, where normalization consists of dividing the production value by the historical regional monthly average. Normalizing allows to correct for the size effect stemming from regional heterogeneity in production. We refer to Online Appendix A.1 for more details.

Regional Weather Data. Gridded monthly temperature data are sourced from PISCOt V1.1, and precipitation data from PISCOp V2.0, both provided by SENAMHI (the National Service of Meteorology and Hydrology of Peru). The data processing begins by aggregating daily grid-level temperature and precipitation to a monthly basis. Given crops' sensitivity to extreme daytime conditions (Parry et al., 2007), we use average monthly maximum temperature as a key predictor, alongside a precipitation amount indicator. Following D'Agostino and Schlenker (2016), weather data are first processed at the grid cell level and then aggregated to a monthly regional scale. The next step is to calculate weather shocks as deviations of temperature and precipitation from their 30-year historical averages, therefore constructing weather anomalies, following standard practices (Deschênes and Greenstone, 2007; Auffhammer et al., 2013). More specifically, as in Barrios et al. (2010) we demean grid-level weather data using monthly historical values. The resulting anomalies are then averaged across grid cells within each region, weighted by the region's area and agricultural production. This process yields region-specific temperature and precipitation anomalies, which represent deviations from long-term normals. The detailed aggregation process is described in the Online Appendix.

ENSO Oscillations. To explore the cause-and-effect relationship, local projections are typically built under the assumption that weather shocks are unexpected. However, our sample also includes El Niño and La Niña events. These climate phenomena are characterized by their predictable occurrence, diverging from the typical unexpected nature of weather shocks.[11] To overcome this issue, we use ENSO variations as a control variable to account for the expectational effect that ENSO may have on the projection. These ENSO fluctuations are classified using the Oceanic Niño Index. We collect this index from the Golden Gate Weather Service.

[11]Even though farmers are still surprised by the magnitude of the weather shocks during ENSO events, they can adapt by adjusting their crop mix before the weather shock materializes, introducing a potential bias in the quantitative analysis.

Macroeconomic Data. To isolate the pure effect of weather shocks,[12] we control for macroeconomic conditions using the data warehouse of *the Banco Central de Reserva del Peru*.[13] The following series are included: the Peruvian Consumer Price Index (CPI), Food Price Index (FPI), PEN/USD Exchange rate, national interest rate, GDP index and a sectoral index for industrial production. Note that all the control variables are national aggregates given on a monthly basis. Nominal variables (*e.g.*, exchange rate, FPI, and CPI) are detrended by calculating their growth rate. GDP, industrial production indices and interest rate data are detrended via Hodrick-Prescott filter. In addition, we control for international variations that may affect the production of each culture by including their respective commodity prices using IMF data.

2.2 Summary Statistics of Agricultural Data

Table 1 presents descriptive statistics for the monthly production of the selected crops averaged over the regions. Significant variations in production are observed, and these variations are highly crop-specific. It displays the mean, median, standard deviation, minimum, and maximum production values in tons, along with the mean and maximum growth duration (in months) for each crop. The table also includes the number of regions where each crop is grown and the total number of observations.

	Regional Production (tons)					Growth Duration			
Culture	Mean	Median	Std Dev.	Min.	Max.	Mean	Max.	No. regions	No. obs.
Cassava	4,531	1,799	7,110	0	57,135	9	14	20	3,600
Maize	4,291	983	7,255	0	74,624	5.17	12	23	4,140
Potato	16,393	5,049	29,575	0	360,070	5.79	8	19	3,420
Rice	13,458	1,654	28,313	0	318,706	4.44	6	16	2,880

Notes: Each region contains 180 observations, from January 2001 to December 2016. Duration is expressed in months. 'Std Dev.' stands for standard deviation. Source: MINAGRI. Author's estimate

Table 1. Descriptive Statistics for Monthly Production (in Tons) per Type of Crop.

In terms of production quantity, potato and rice stand out as the largest crops, with average monthly regional outputs of 16,393 and 13,458 tons, respectively, far exceeding those of

[12]Because the data-generating process of our agricultural data is driven by alternative sources of randomness, such as economic shocks unrelated to the weather, we include macroeconomic data as control variables. The goal of these control variables is to isolate the effect of weather variables on agricultural production from any other sources of fluctuation. By holding constant values for the control variables, any changes in the outcome can be attributed solely to the variable of interest, rather than the combined effects of multiple variables. This makes it possible to draw more accurate conclusions regarding the causal relationship between weather shocks and agricultural output.

[13]Data are taken from the Central Bank of Peru, where the Real Exchange Rate token is *PN01259PM*, Exports is *PN01461BM*, Food CPI is *PN01336PM*, CPI is *PN01270PM*, industrial GDP is *PN02079AM*, GDP *PN01773AM*, and interest rate is *PN07819NM*. All seasonal components are removed from the time series, excluding the interest rates.

cassava and maize. Potato and rice exhibit much higher relative volatility, as reflected in their larger standard deviations relative to their means. For example, rice has a standard deviation of 28,313 tons compared to a mean of 13,458, indicating significant production fluctuations. Similarly, potato, with the largest standard deviation of 29,575 tons, shows greater variability in production compared to cassava and maize, whose standard deviations are relatively lower in proportion to their means. This suggests that potato and rice face greater production risks and variability, possibly due to differences in growing conditions or susceptibility to weather shocks.

3 The Dynamic Effects of Weather Shocks

How do weather shocks dynamically affect agricultural production? This section discusses the econometric approach and the main results obtained from the impulse response function analysis.

3.1 Empirical Approach

We base our empirical framework on a conceptual framework similar to that developed by Dell et al. (2012). To fix ideas, consider the following simple economy characterized by a Cobb-Douglas technology in the agricultural sector in region i for crop c:

$$Y_{c,i,t} = A_{c,i} N_{c,i,t} H_{c,i,t}, \tag{1}$$

where the agricultural output for crop type c planted in region i at time t is denoted by Y, crop-regional total factor productivity is denoted by A, labor demand is denoted by N and harvested area is denoted by H. Note that in this expression, $A_{c,i}$ captures how regional conditions, such as local labor productivity, shape the productivity of labor for crops planted in this region. By contrast, $N_{c,i,t}$ encapsulates macroeconomic fluctuations stemming from the labor market (*e.g.*, all aggregate shocks realized in t determine the country-wide real wage). Finally, $H_{c,i,t}$ represents the surface harvested with N units of labor.

How does the weather interfere within the production process of agricultural goods? Consider that each period, farmers in region i plant crop c on land surface L. A typical crop growth cycle implies a lag between planting and harvesting, referred to as the *growing season*. During the growing season, crops are vulnerable to weather shocks such as droughts and floods, leading to reduced growth and yield. In addition to these direct effects, weather shocks lead to increased stress in plants, making them more vulnerable to diseases. In severe cases, droughts can cause complete crop failure.

To capture these delayed effects of the weather on agricultural yields, let T_c denote the monthly duration of the crop-specific growing season between planting ($h = 0$) and

harvesting ($h = T_c$). Therefore, it is assumed that $L_{c,i,t}$ units of planted land yield $L_{c,i,t} \exp(\sum_{h=0}^{T_c} \alpha_{c,h} W_{i,t-h})$ effective units of productive land, where a weather shock $W_{i,t-h}$ realized in $t-h$ affects crop production harvested in t with elasticity $\alpha_{c,h}$.[14] Weather shocks are considered from the farmer's perspective as exogenous variables that affect land productivity during the growing season. Weather variables, stacked in W, are formally connected to agricultural output as follows:

$$H_{c,i,t} \leq L_{c,i,t} \exp\left(\sum_{h=0}^{T_c} \alpha_{c,h} W_{i,t-h}\right). \tag{2}$$

In this expression, it is assumed that the land surface planted $L_{i,c,t}$ exhibits both seasonal and trend components stemming from soil quality across time and space. Assuming that all planted surfaces are harvested, Equation 2 holds with equality. However, in the presence of severe weather shocks, if the marginal cost of harvesting exceeds the marginal profits of the land, it might be optimal for farmers to partially harvest the planted surface.

Combining Equation 1 and Equation 2, and applying logs yields the following expression:

$$\ln\left(\frac{Y_{c,i,t}}{L_{c,i,t}}\right) = \ln\left(A_{c,i}\right) + \sum_{h=0}^{T_c} \alpha_{c,h} W_{i,t-h} + \ln\left(N_{c,i,t}\right). \tag{3}$$

The left-hand side of this equation represents the percentage deviation of agricultural production from its potential value, measured by $L_{c,i,t}$. Note that one can express the logarithm into a percentage deviation of $Y_{c,i,t}$ from $L_{c,i,t}$ as follows: $y_{c,i,t} = \ln(Y_{c,i,t}/L_{c,i,t})$ to be consistent with the local projection.

A natural question at this stage is to gauge the importance of the elasticity of agricultural production to changes in weather conditions, namely, to infer the value of $\alpha_{c,h}$. We use local projections based on Jordà (2005) to estimate the impact of weather shocks on agricultural output during the crop growing season. LPs are an econometric technique used to estimate the dynamic response of an outcome variable to an exogenous shock.[15] In this study, the two main exogenous variables are precipitation and temperature anomalies described in the data section.

LPs are easy to implement, requiring a series of regressions—one for each forecast hori-

[14] Note that we do not include a squared value for the weather variables. Squared terms are typically introduced to capture low-frequency effects of climate change. In this study, the time-frequency is monthly. The use of a squared term does not change the sign or significance of the results, as can be observed in the online replication materials.

[15] Unlike traditional VARs, LPs do not require the estimation of the entire autoregressive structure of the data. Instead, LPs estimate the response of the dependent variable directly for each forecast horizon using linear estimation techniques. Impulse response functions are obtained without imposing a specific parametric form on the entire time series process and can accommodate various types of shock specifications and controlling variables.

zon. For each horizon h, the dependent variable is regressed on the shock variable and other controls, capturing the direct impact at that specific horizon. Compared to VAR, LPs are robust to model misspecifications. Since each horizon is estimated separately, errors in one horizon do not propagate to others. Additionally, LPs do not require strong exogeneity assumptions, which are often needed in VAR models.

To estimate these effects, for each crop c, we run a local projection for $h = \{0, 1, ..., T_c\}$ of the form:

$$\begin{aligned} y_{c,i,t+h} =& \alpha^T_{c,h} T_{i,t} + \alpha^P_{c,h} P_{i,t} + \beta_{c,i,h} X_t \\ &+ \gamma_{c,i,h} \text{Trend}_t \times \text{Month}_t + \delta_{c,i,h} \text{Trend}^2_t \times \text{Month}_t + \varepsilon_{c,i,h}, \end{aligned} \tag{4}$$

where h is the time horizon. Agricultural production $y_{c,i,t+h}$, is normalized with respect to the long-term average (see Equation OA.2 in the Online Appendix). To account for a possible trend in the potential production of crops measured by $L_{c,i,t}$ in Equation 3, a month- and region-specific quadratic trend is included in the equation, in the same spirit as Gammans et al. (2017).[16] The associated coefficients, $\gamma_{c,i,h}$ and $\delta_{c,i,h}$ need to be estimated. The terms $T_{i,t}$ and $P_{i,t}$ represent the two distinctive weather variables that are considered in the inference exercise, namely, the temperature and precipitation anomaly variables (as detailed in Online Appendix A.2).[17] The two sequences of coefficients associated with the weather variables, $\alpha^T_{c,h}$ and $\alpha^P_{c,h}$, are of first-order interest as they indicate how sensitive agricultural output is to exogenous changes in the weather variables.

In addition, $X_t = [RER_t, r_t, \pi_t, y^{\text{ind}}_t, ENSO_t, \pi_{c,t}]$ is the set of control variables that captures the contributions from aggregate fluctuations, as stacked in the labor demand term in Equation 3. The control variables include the Real Exchange Rate (RER_t) and the nominal interest rate (r_t), both expressed as the deviation from the trend calculated by the Hodrick-Prescott filter, the inflation rate (π_t), the seasonally adjusted industrial production index (y^{ind}_t) expressed as a percentage deviation from the trend calculated by the Hodrick-Prescott filter, the Oceanic Niño Index ($ENSO_t$), and the monthly international price variation of each crop ($\pi_{c,t}$). The set of coefficients $\beta_{c,i,h}$ is unknown and must be estimated in the inference exercise. Finally, $\varepsilon_{c,i,t+h}$ is an error term assumed to be normally distributed with zero mean.

3.2 Impulse Response Functions Results

The estimated coefficients $\alpha^T_{c,h}$ and $\alpha^P_{c,t}$ in Equation 4 are multiplied by the standard deviation of the weather variable to obtain the impulse response of agricultural production to a standard weather shock. The responses are reported in Figure 1 for a fourteen-months horizon, contrasting the four different crops considered. The horizon is chosen based on the

[16] The $\texttt{Month}_t$ term is a matrix of monthly dummy variables.

[17] See Appendix B for alternative definitions of the weather shocks.

longest estimated growth duration among the crops (which is 14 months maximum for cassava; see Table 1). To facilitate a clearer interpretation of the figures, we use the same horizon for all crops. However, since the growth duration is specific to each crop, we represent the average season duration on the graphs with an orange dashed vertical line. A response to a one standard deviation shock of temperature anomalies is reported at the top and for precipitation anomalies at the bottom.[18] In both cases, a positive shock is considered: a one standard deviation increase in temperature and a one standard deviation increase in precipitation, both with respect to their historical averages. Positive deviations in temperature or precipitation anomalies correspond to higher-than-usual values.[19]

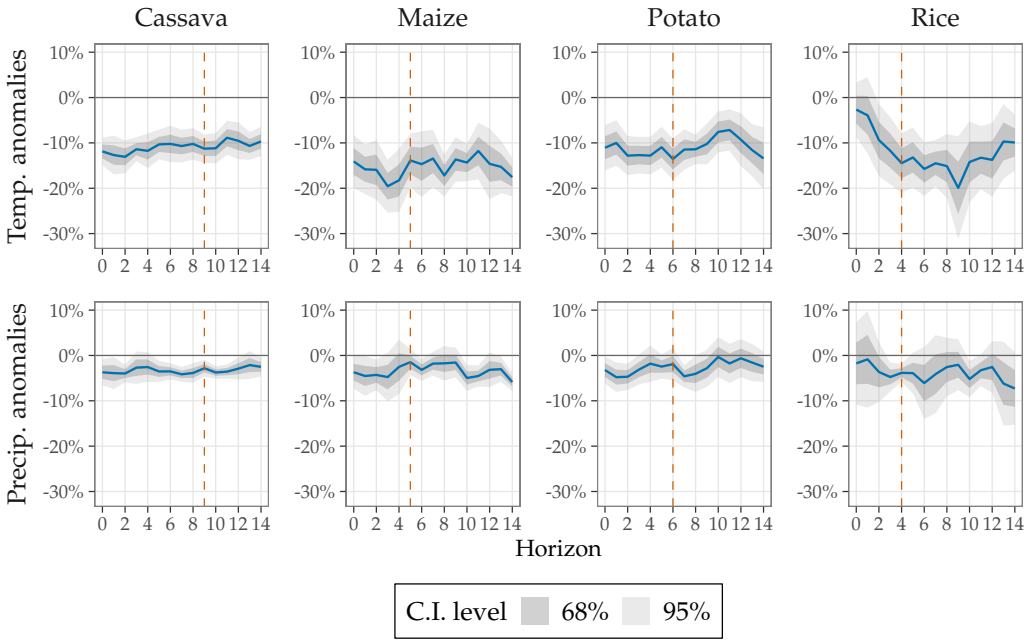

Notes: The panels show the crop-specific impulse response function of monthly agricultural production to a one standard deviation (SD) increase in the weather variable, which is defined as a 1 SD increase with respect to the historical average. The weather variables are the temperature anomaly in the first row and the precipitation anomaly in the second row. Horizon 0 represents the month of the shock. The shaded areas represent the 95% and 68% confidence intervals with region-level clustered standard errors. The orange dashed bars represent the average growth duration.

Figure 1. Agricultural Production Response to a Weather Shock.

Overall, the shock leads to a sharp and net decrease in production for several months for every crop considered in our sample. However, the response is crop-specific due to the heterogeneous characteristics of the four types of crops considered. In terms of magnitude, maize production appears to be the most affected by a temperature shock, with a loss of 15% of the detrended production after a rise in the monthly maximal temperatures of one standard deviation with respect to the historical average. The effect of the shock lasts for several months, and production remains highly altered even months later. Rice exhibits a smaller

[18] Note that the number of regions is not the same across crops because some regions do not produce specific types of agricultural products. We refer to Table 1 for a description of agricultural production per region and crop type.

[19] Differential effects based on the sign of the anomaly are discussed in Appendix B.

response on impact, suggesting that this crop type is more temperature-tolerant one or two months before harvesting. However, this response is followed by a gradual drop in production that lasts longer than the crop's growth period. Note that IRFs not necessarily returning to zero after harvesting underscores hysteresis mechanism.[20] We attribute hysteresis to several factors. Possible explanations include reduced income, depletion of inputs, delays in reallocating land or resources, and shifts in the composition of farmers within a region. This result suggests a learning mechanism, where farmers adapt their crop selection in future growing seasons.

The second row of panels in Figure 1 reports the response of agricultural production following the realization of a precipitation anomaly shock at $h = 0$. A positive realization of the shock is associated with wetter-than-usual weather, specifically, a one standard deviation increase in total precipitation relative to the historical average. A precipitation anomaly exhibits a similar pattern to temperature anomaly shocks but with a response of relatively smaller magnitude. Excess rainfall is detrimental to agricultural production, leading to an average agricultural loss between 2% and 8%, with stronger effects occurring a few months after the shock. As explained by Skees et al. (2007), excess rainfalls—such as those driven by El Niño events in Peru—devastated several regions with massive flooding that washed crops away.[21] The presence of a tropical climate, characterized by abundant rainfall, induces a large decrease in agricultural production following the realization of the precipitation anomaly shock. Although the shocks display a similar pattern, each crop reacts differently to them through the timing and magnitude of their responses.

Variations in production following a precipitation shock are also highly crop-specific and more volatile than responses to temperature shocks. Cassava, maize, and potato are clearly affected during the first months following the shock, with the effect becoming more variable and less significant over time. In contrast, rice is sensitive to precipitation, but the impact is observed two months after the realization of the shock. Notably, for potato and rice, the effects of the precipitation tend to vanish as the horizon grows, while cassava and maize exhibit more persistent effects. This persistence highlights that farmers tend to lower production even after the crop growth duration, indicating an adaptation mechanism.

4 Time-varying Exposure to Weather Shocks

The baseline projections in section 3 underline that the effects of weather shocks are heterogeneous over the horizon of the IRF. These abnormal weather shocks have immediate

[20] It is not surprising for impulse response functions in local projections to not return to zero, as they can capture persistent or long-term effects of shocks that may not fully dissipate over the projected time horizon. In the canonical paper of Jordà (2005), the IRFs also do not converge to zero.

[21] Crost et al. (2018) find that an increase in wet-season rainfall is harmful to crops and produces more conflict in the Philippines.

impacts, but also delayed effects, implying that not only the crops ready to be harvested but also those that are still in their early growing stages are affected. Thus, a natural question that arises from this observation is to investigate the time-dependence of weather shocks over the growing stages of crops.

A significant body of literature has already demonstrated that the impact of weather shocks on agriculture significantly depends on crop growth stages. For instance, Welch et al. (2010) show differential effects of increases in minimum and maximum temperatures on rice yields in tropical/subtropical Asia based on the growth phase. Additionally, Letta et al. (2022) find that weather shocks trigger a rise in food prices during the growing period. Moreover, Massetti et al. (2016) empirically examine how weather shocks during a growing season affect maize and soybean harvests using US county-level data. Crops necessitate different types of nutrients depending on the stage of plant development. Excessively high temperatures or water volumes can be highly detrimental to crop growth at some stages while having little or no effect at other stages.

This section aims to capture this effect. We take advantage of the high frequency of the data to monitor the quantity of crops planted and harvested each month. Departing from the conventional approach in the literature, which often uses fixed periods to define growth and harvest seasons, our methodology involves a monthly continuous variable that weighs the flow of land planted versus harvested. This enables a more dynamic assessment of agricultural stages, distinguishing between the growing period (*i.e.*, when the planted surface is increasing) and the harvesting period (*i.e.*, when the harvested surface is increasing). The response of agricultural production to weather shocks can be contrasted between planted and harvested regimes. To achieve this using local projections, we adapt the framework developed by Auerbach and Gorodnichenko (2011) for fiscal policy, modifying it to accommodate state-dependent effects of the weather with a smooth transition between the growing and harvesting stages. This framework enables us to empirically track the variation in the start and duration of the growing and harvesting seasons, rather than fixing them arbitrarily as done in most literature. Instead, having flexible seasons allows to account partially for farmers adjustments, who could adapt their practices in the context of climate change (Cui and Xie, 2022).

4.1 A State-dependent Framework

Based on the previous toy model of agricultural production from Equation 2, we modify this model to formalize plant cycles and the underlying time-varying sensitivity of land productivity to weather shocks.

Let $p_{c,i,t}$ denote the new surface planted and $h_{c,i,t}$ denote its harvested counterpart at time t for crop type c in region i. Therefore, the net flow of the newly planted surface is

given by $p_{c,i,t} - h_{c,i,t}$. The total fraction of land with growing crops is measured here as the cumulative sum of flows in the cultivated land surface over the lifetime of a crop T_c as follows: $z_{c,i,t} = \sum_{h=0}^{T_c}(p_{c,i,t-h} - h_{c,i,t-h})$. To compare regions on a regular basis, we remove the possible trend and divide by the standard error as follows, $\hat{z}_{c,i,t} = (z_{c,i,t} - z_{c,i,t}^{HP})/\sigma_{c,i,t}$, where $\hat{z}_{c,i,t}$ is the zero-mean standardized index variable of the utilized land surface. To express this index as a transition function with support $[0, 1]$, since the planted surface index has been standardized, $\hat{z}_{c,i,t} \sim \mathcal{N}(0, 1)$, we use the cumulative distribution function of the standard normal distribution $\Phi(\cdot)$:[22]

$$\Phi(\hat{z}_{c,i,t}) = \frac{1}{\sqrt{2\pi}} \int_{-\infty}^{\hat{z}_{c,i,t}} \exp(-t^2/2)\, \mathrm{d}t. \tag{5}$$

Letting $\Phi(\hat{z}_{c,i,t})L_{c,i,t}$ denote the fraction of the potential land that is planted, $\Phi(\hat{z}_{c,i,t})$ is interpreted as the mass of land planted or the degree of exposure of agricultural production to weather changes.

Consider now that weather effects depend on the growth stage of crops. The harvesting season is interpreted as the period when the mass of land planted $\Phi(z_{c,i,t})$ is low (approaching zero). By contrast, the growing season corresponds to a situation in which $\Phi(z_{c,i,t})$ is high (approaching one). Differentiating the effects of the weather on the growing and harvesting seasons, the surface of harvested land can be written as follows:

$$H_{c,i,t} \leq L_{c,i,t} \exp\left(\sum_{h=0}^{T_c} \left(\Phi(\hat{z}_{c,i,t-h})\alpha_{c,G}^{h} + (1 - \Phi(\hat{z}_{c,i,t-h}))\alpha_{c,H}^{h}\right) W_{i,t-h}\right), \tag{6}$$

where $\alpha_{c,G}^{h}$ and $\alpha_{c,H}^{h}$ are agricultural production responses during the growing and harvesting seasons, respectively.

Injecting this term into the production yields the following expression:

$$\ln\left(\frac{Y_{c,i,t}}{L_{c,i,t}}\right) = \ln\left(A_{c,i}\right) + \sum_{h=0}^{T_c} \left(\Phi(\hat{z}_{c,i,t})\alpha_{c,G}^{h} + (1 - \Phi(\hat{z}_{c,i,t}))\alpha_{c,H}^{h}\right) W_{i,t-h} + \ln\left(N_{i,c,t}\right). \tag{7}$$

The local projections framework can be adapted again to analyze the role of the growing versus harvesting season in the propagation of shocks. We examine the non-linear influence of the season on the response of each crop production to weather shocks. The same local projection method is used, but augmented with a state-dependent variable to allow for non-linear responses as described in Auerbach and Gorodnichenko (2011). This framework considers the

[22] Note that Auerbach and Gorodnichenko (2011) adopt a similar strategy to define recessions but assume a logistic transition function, which implies having to arbitrarily define a threshold when calibrating the parameters of the logistic function. To avoid this assumption, we use the cumulative distribution function of the standard normal distribution, which in turn is more agnostic with respect to the transition.

probability of being in the growing season or during the harvesting season:

$$
\begin{aligned}
y_{c,i,t+h} = \Phi\left(\hat{z}_{c,i,t}\right) \Big[& \alpha_{c,h}^{G,T} T_{i,t} + \alpha_{c,h}^{G,P} P_{i,t} + \beta_{c,i,h}^{G} X_t + \gamma_{c,i,h}^{G} \text{ Trend}_t \times \text{Month}_t \\
& + \delta_{c,i,h}^{G} \text{Trend}_t^2 \times \text{Month}_t \Big] \\
& + \left(1 - \Phi\left(\hat{z}_{c,i,t}\right)\right) \Big[\alpha_{c,h}^{H,T} T_{i,t} + \alpha_{c,h}^{H,P} P_{i,t} + \beta_{c,i,h}^{H} X_t + \gamma_{c,i,h}^{H} \text{Trend}_t \times \text{Month}_t \\
& + \delta_{c,i,h}^{H} \text{Trend}_t^2 \times \text{Month}_t \Big] + \varepsilon_{c,i,t+h}, \qquad (8)
\end{aligned}
$$

where $y_{c,i,t+h}$ is the deseasonalized production, and $T_{i,t}$, $P_{i,t}$, and X_t are, respectively, the temperature anomalies, precipitation anomalies, and control variables, as previously defined in Equation 4. Again, a monthly region-specific quadratic trend is included in the model. The difference from this latter equation is that we now estimate the associated coefficients conditionally on the state of the season. Note that $\alpha_{c,h}^{H,T}$ and $\alpha_{c,h}^{H,P}$ are, therefore, the parameters of interest for the harvesting season, whereas $\alpha_{c,h}^{G,T}$ and $\alpha_{c,h}^{G,P}$ are the parameters for the growing season. Following Auerbach and Gorodnichenko (2011), we also allow for seasonally dependent fixed effects and marginal effects for the control variables.

4.2 Season-dependent Impulse Response Functions

The response obtained from Equation 8 are reported in Figure 2. As before, the first row presents the crop-specific responses to a one standard deviation temperature anomaly shock, whereas the second row shows the responses to a precipitation anomaly shock. Responses are distinguished by regime: the gray line represents the responses during the growing season, while the green line refers to the harvesting season. Confidence intervals are reported at the 95% confidence level.

The distinction between growing and harvesting seasons plays an important role. Overall, we observe a differentiated impact, with a stronger reduction in production when a shock occurs during the growing season. This result appears more clearly when examining temperature shocks, whereas precipitation shocks display a more volatile response.

Two results are important to notice with this specification. First, looking at the responses to temperature shocks, we observe that both the magnitude and duration of the shock differ depending on its timing. Using the example of cassava and rice, we discern two specific patterns. When a temperature shock happens during the growing season, while production decreases instantaneously, the strongest reduction occurs several months after the shock. This result suggests that a shock affects both mature crops (immediate effect on production) and, with a delay, crops that are in their growth phase at the time of the shock. This result is in line with Hatfield and Prueger (2015) who find that when a temperature shock occurs during the growth stage of crop development, it may affect crop growth, which in turn leads to lower yields. However, if a shock occurs when the crop is about to be harvested, then only a high-

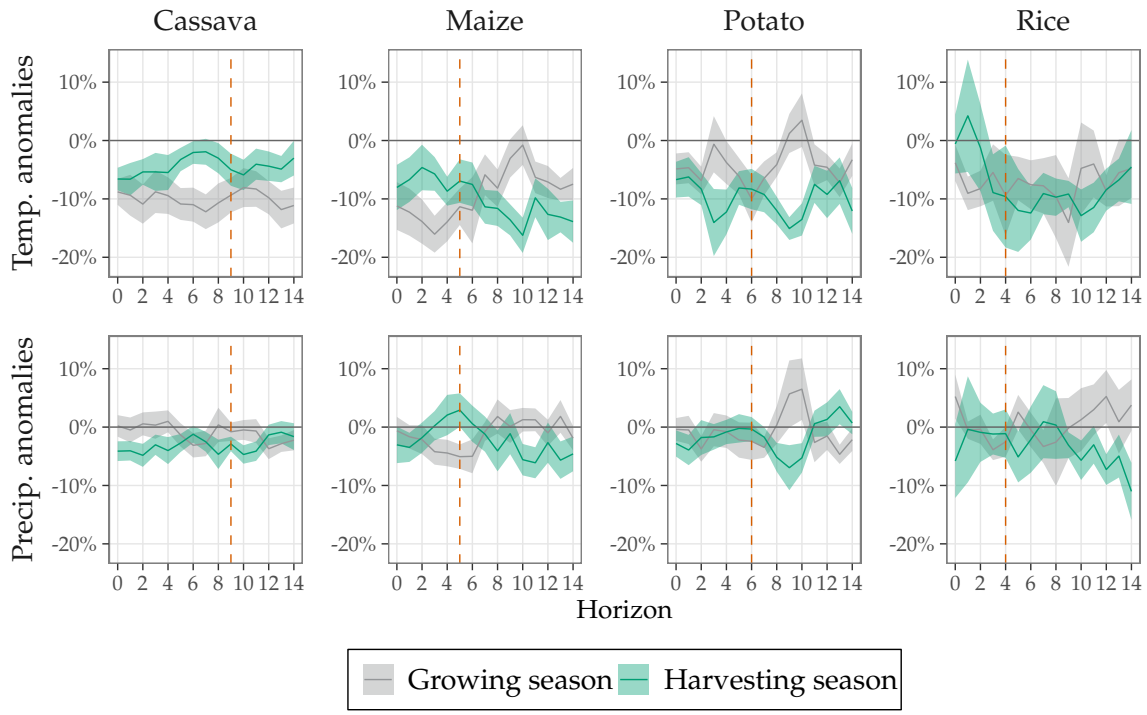

Notes: The panels show the crop and season-specific impulse responses of monthly agricultural production to a 1 SD increase in the weather variable. The weather variables are the temperature anomaly in the first row and the precipitation anomaly in the second row. Horizon 0 represents the month of the shock. The bands formed by the grey and green areas represent the 95% confidence intervals with standard errors clustered at the regional level for the growing season and harvesting season regimes, respectively. The orange dashed bars represent the average growth duration.

Figure 2. Agricultural Production Response to a Weather Shock Contrasting for Growing vs. Harvesting Season.

magnitude shock (*e.g.*, severe drought, hail, landslide, etc.) is likely to significantly affect production. The response of cassava production shows that the detrimental effect is smaller in magnitude and duration compared to growing season shocks. In the case of rice, a positive—yet non-significant—response of production after a temperature shock is observed, which may be driven by better drying conditions for grains.

Strikingly, this effect of temperature shocks is common to all crops except potatoes, although its timing and duration remain highly crop-specific. Precipitation shocks lead to more volatile and less significant responses. This underscores the importance of considering the different effects of the season, which may not appear clearly when looking at aggregated variations over time. Because the seasons may vary slightly between regions (see Figure OA.4), estimating the aggregated effect of weather shocks, as in section 3, may undervalue the duration of the shock and thus provide a lower bound of the potential regional effects. Given that the responses differ with respect to season, policies designed to mitigate the aftermath of a shock should be adapted accordingly.

5 From Regional to Country-Wide Fluctuations

Are regional weather shocks sufficiently important to spread to the rest of the economy? Weather shocks tend to be serially correlated across regions because these regions share common atmospheric, soil, or topographic patterns. Therefore, a weather shock may entail macroeconomic fluctuations at the national level if the number of regions affected by the same weather pattern is high enough. On policy grounds, a quantitative assessment of weather shocks to macroeconomic fluctuations is particularly important for the design of mitigation policies.

In what follows, we first extract a national aggregate index of the weather shocks on agricultural output. We next propose to analyze the aggregate effects of weather shocks through the lens of local projections and a VAR framework. VAR are a widespread tool in macroeconometrics for forecasting purposes, and (unlike local projections) amenable for counterfactual policy analysis.

5.1 A National Measure of Weather Damages: the Weather Component of Agricultural Loss (WCAL)

The literature typically provides a synthetic measure of weather based on average measures of county-level weather shocks and analyzes its interaction with macroeconomic time series (see, *e.g.*, Natoli, 2024; Gallic and Vermandel, 2020). This approach typically infers an immediate effect of a contemporaneous weather shock in t on macroeconomic variables, and its delayed reverberation through the propagation patterns over $t + N$ with an N horizon. This methodology arbitrarily forces weather shocks to have immediate and homogeneous impacts on agricultural production, underestimating both (i) the delayed effects from the crop growth process and (ii) the heterogeneous responses of different crops.

By contrast, we propose measuring the macroeconomic effects of the weather through a "weather-implied losses" variable, as measured by our baseline local projections in Equation 4. We define the national weather-adjusted agricultural production y_t^{ω} at time t by summing the significant crop-specific contributions of weather represented by the coefficients of the weather variables $\beta_{c,h}^{T}$ and $\beta_{c,h}^{P}$ over the horizons and regions:[23]

$$y_t^{\omega} = \frac{1}{\sum_c \omega_{c,t}} \sum_c \sum_h \sum_i \frac{\mathbb{1}_{\text{signif}_{c,i,t,h}} \times \left(\beta_{c,h}^{T} T_{i,t-h} + \beta_{c,h}^{P} P_{i,t-h}\right) \times \omega_{c,t}}{\text{card}(I_{c,t})}, \tag{9}$$

where $\omega_{c,t} = \sum_i y_{c,t,i}^{\text{raw}} \times p_c$ is a quantity weight for crop c at time t. It represents the sum of monthly agricultural production over regions, expressed in monetary terms, where p_c is the average selling price of crop c in our sample. $\text{card}(I_{c,t})$ is the number of regions that produce

[23] The steps to obtain the expression of this variable are detailed in Online Appendix B.

crop c at time t, and the characteristic function $\mathbb{1}_{\text{signif}_{c,i,t,h}}$ equals 1 when the contribution is significantly different from 0 (based on the 95% confidence intervals of the coefficients $\beta^T_{c,h}$ and $\beta^P_{c,h}$), and 0 otherwise. The horizon h retained here to define the indicator is 9 months, corresponding to the longest average growth duration among the four crops studied (see Table 1). This choice focuses on the surprise element of the shock, and avoids encompassing adaptive responses that might occur over a longer horizon.

The national weather-adjusted agricultural production is then expressed as a measure denoted WCAL_t, termed the "weather component of agricultural losses," measured in percentage deviations from trend:

$$\text{WCAL}_t = -100 \times (y^{\omega}_t - \overline{y^{\omega}_t}). \tag{10}$$

This metric represents the deviation or loss from the expected trend. The trend itself is determined through the application of a Hodrick-Prescott filter. The inclusion of a negative sign ensures that positive values of WCAL_t correspond to losses, rather than gains. In simpler terms, WCAL_t provides an intuitive measure that expresses the percentage loss of agricultural value-added attributed to weather shocks.

5.2 Quantitative analysis

In this section, we measure the country-level effect of weather shocks through our new synthetic measure of weather shocks. We employ Vector Auto Regressive (VAR) and local projections (LP) to measure the propagation of weather losses at the national level of Peru. A methodological description is given in Appendix D for VAR and LP. The vector of endogenous variables, $Y_t = \left[\text{WCAL}_t,\ \text{RER}_t,\ \pi^A_t,\ \pi_t,\ X_t,\ y^A_t,\ y_t,\ r_t\right]$, contains eight variables: the aggregate measure of weather-driven agricultural losses denoted WCAL_t, Real Exchange Rate denoted RER_t, the percentage change in the Food Consumer Price Index denoted π^A_t, the percentage change in the Consumer Price Index (CPI) denoted π_t, exports denoted X_t, agricultural production denoted y^A_t, GDP denoted y_t and nominal rate r_t. All macroeconomic data are presented in the data section, except for the agricultural output, which is calculated using the regional monthly production values for the crops of interest $y^A_t = \sum_c \omega_{c,t}$, where $y^{\text{raw}}_{c,t,i} \times p_c$ is the quantity weight for crop c at time t from the local projection. Variables exhibiting a trend (agricultural output and GDP) are expressed as percentage deviations from the Hodrick-Prescott trend, while seasonal components are removed using the X13 method of the Census Bureau. Our sample covers the period 2003M1–2015M12.

With the Cholesky factorization of the reduced-form VAR covariance matrix, the order of the variable matters. To impose full exogeneity in the weather process, we follow Gallic and Vermandel (2020) by placing the weather-driven agricultural-losses equation in the first position in the VAR and muting cross-interactions with other variables. Following the ordering scheme of Stock and Watson (2001), we next order price variables, followed by quantities,

and terminate with interest rates. The idea is that price variables are driven more by exogenous factors (*e.g.*, oil price shocks), whereas the interest rate is the most endogenous variable that reacts to contemporaneous changes in prices and quantities.

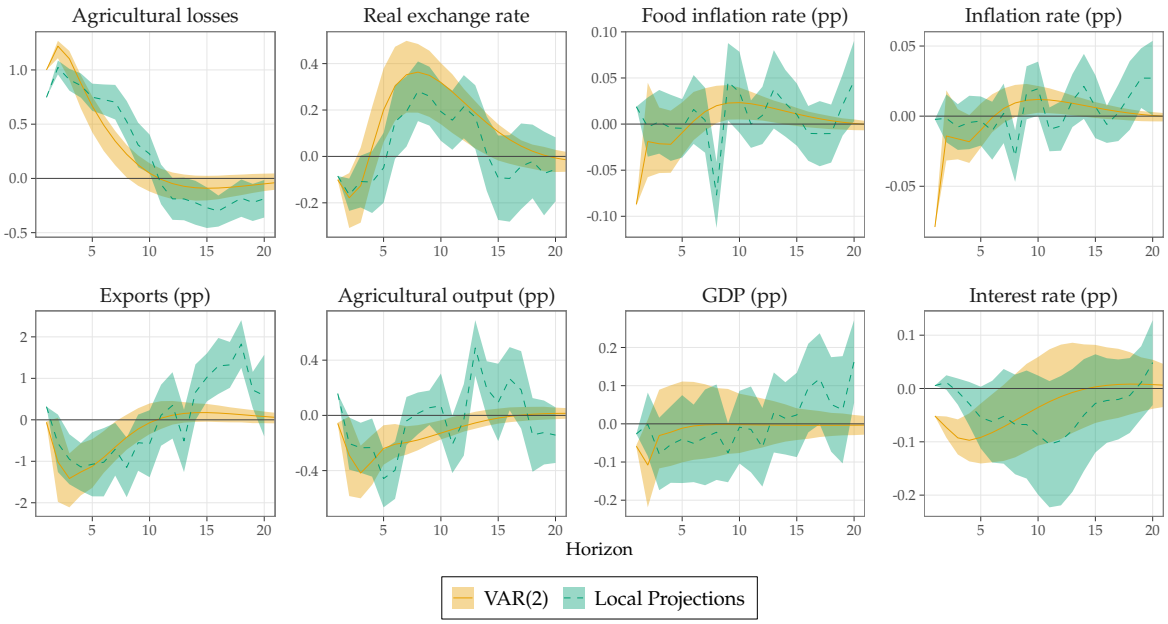

Notes: The solid yellow lines represent the Impulse Response Function (IRF) obtained from the VAR model, and the yellow areas correspond to the 68% confidence interval. The green dashed lines draw the IRF obtained from the Local projection model and the green area are the corresponding 68% confidence intervals. The response horizon is in months, and Horizon 0 represents the month of the shock.

Figure 3. System Response to a Unit Orthogonal Shock to the Weather Aggregate Cost Equation.

The number of lags selected using the AIC criterion is 2. Figure 3 illustrates the system's response to a unit increase in agricultural output resulting from weather shocks. This section primarily focuses on the results of the VAR, as these results are typically easier to interpret. LPs are included to provide robustness to the results by offering an alternative assumption on the data-generating process, but IRF are typically much harder to interpret because these responses are not necessarily stationary and smooth.

An increase in losses in the agricultural sector due to weather shocks triggers an immediate 0.1% reduction in the real exchange rate, primarily because exports and output in the agricultural sector decrease. As exports return to their long-term mean, real exchange rates adjust by increasing in response to growing exports. This overall recessionary impact initially leads to decreases in both consumer and food price indices, reflecting weak demand. This disinflation can be rationalized within a forward-looking standard New Keynesian Phillips curve in open economies: on impact, domestic producers anticipate that the domestic currency will appreciate in the future, lowering future marginal costs and hence inflation today. This disinflationary effect of weather shocks aligns with the findings of Natoli (2024) and Faccia et al. (2021), both of whom observe lower-than-usual inflation following a temperature

shock. However, it is important to note that our setup implies positive inflation 10 months after the realization of the weather loss, which can be attributed to the scarcity of agricultural products and the decrease in real exchange rates, making imports more expensive in the future.

In terms of quantities, a unit loss shock resulting from the weather implies a 0.41% reduction in agricultural output below its trend, while GDP is 0.1% lower. Finally, the central bank faces no trade-off on impact, as both prices and quantities are moving in the same direction. However, after one year, when inflation picks up, a typical supply-driven trade-off emerges between inflation and quantity stabilization, as both move in opposite directions in the medium term. The VAR model suggests that the Peruvian central bank prioritizes output stabilization when weather shocks occur, leading to an accommodative response in the nominal interest rate.

Much of the divergence between local projections concerns price dynamics, which consequently affect the response of monetary policy. According to local projections, food and overall inflation decline 7 months after the realization of the shock, leading to delayed effects on interest rates. Note also that the IRFs for inflation and exports do not necessarily go back to zero. This is not surprising: local projections are not constrained by stationarity, which contrasts with the assumptions typically imposed in VAR models. While VARs require weak stationarity, LPs are more flexible and agnostic, accommodating a wide range of data-generating processes, including those with non-stationary dynamics.

To connect our work with prior studies, our quantitative assessment of the macroeconomic cost of weather shocks aligns with existing literature. The responses of output and interest rates closely mirror the findings of Natoli (2024) for the US economy regarding temperature anomalies. Additionally, our results are consistent with the VAR model of Gallic and Vermandel (2020) for New Zealand, where they similarly observe a 0.1% decrease in GDP, a 1% decline in agricultural output, and a 0.4% drop in the real exchange rate following a drought shock.

6 Conclusion

This paper provides a quantitative exploration of the impact of weather shocks on agricultural production in Peru, using high-frequency, crop-region-specific data. By employing a linear panel model with local projections, we have quantified the immediate and lagged effects of temperature and precipitation anomalies on various crops. Our findings indicate that weather shocks lead to significant declines in agricultural output, with the magnitude and duration of these effects varying across different crops.

At the macroeconomic level, weather-induced losses in agricultural output translate into

broader economic impacts, including reductions in GDP and potential increases in food prices. Policymakers can use our estimates to anticipate periods of agricultural scarcity and implement measures such as import adjustments to stabilize local markets. Additionally, our study highlights the necessity for adaptive agricultural practices and policies that enhance the resilience of crops to extreme weather conditions, particularly in the context of climate change.

This paper also highlights the importance of employing relatively more disaggregated data to capture the effects of weather shocks and climate impacts more broadly. With longer time-series data, our methodology could be extended to other important research questions, especially those related to the adaptation and mitigation strategies implemented by farmers from a macroeconomic perspective. This, in turn, could be put into perspective with the results from studies using microeconomic data relying on household surveys.

The methodology presented in this paper offers valuable tools for policymakers. By monitoring extreme precipitation and temperature events in specific regions, governments can anticipate their future delayed effects on agricultural production several months in advance. This anticipation can help the implementation of mitigation policies to avoid surges in local food prices.

Future research should aim to integrate our high-frequency analysis with models that account for intertemporal mitigation strategies by farmers. Such integration could provide a more comprehensive understanding of how farmers adjust their practices over multiple seasons in response to weather shocks. Additionally, combining high-frequency production data with household-level surveys could shed light on the impacts of weather shocks on income, consumption, and overall well-being, offering valuable insights into the socio-economic dimensions of climate resilience.

Appendix A Replication Codes

All the codes used to produce this article are available online. We provide an ebook (https://3wen.github.io/weather-peru/) that explains, step by step, how to reproduce the results, using R software. The index of the ebook links to archive files containing the data and the codes.

Appendix B Positive vs. Negative Surprise Weather Shocks

Positive and negative weather shocks may have differentiated impacts on production. The definition of weather shocks in the main part of the paper assumes symmetrical effects. To relax this assumption, we consider, following Natoli (2024), an alternative definition of weather shocks. The idea is to compare the realized temperatures (or precipitation) in a given

month m of year y at location ℓ with expected temperatures (precipitation) based on observations from the same month in previous years at the same location. The difference is defined as a surprise shock.

For days hotter (wetter) than expected, the shock in cell ℓ is defined as:

$$\text{WSurprise}^{(+)}_{\ell,y,m,c} = \underbrace{\sum_{d=1}^{n_m} 1(\mathcal{W}_{\ell,y,m,d} > \text{ut}_{\ell,y,m,c})}_{\text{Climate realization}} - \underbrace{\frac{1}{5}\sum_{k=1}^{5}\sum_{d=1}^{n_m} 1(\mathcal{W}_{\ell,y-k,m,d} > \text{ut}_{\ell,y,m,c})}_{\text{Expected realization}}, \quad \text{(B.11)}$$

where $\mathcal{W}_{\ell,y,m,d}$ is the daily average temperature (or total rainfall), n_m is the number of days in month m, and $\text{ut}^{\ell,y,m,c}$ is the threshold for hot days for crop c.

Similarly, cold (dry) shocks are defined as:

$$\text{WSurprise}^{(-)}_{\ell,y,m,c} = \sum_{d=1}^{n_m} 1(\mathcal{W}_{\ell,y,m,d} < \text{lt}_{\ell,y,m,c}) - \frac{1}{5}\sum_{k=1}^{5}\sum_{d=1}^{n_m} 1(\mathcal{W}_{\ell,y-k,m,d} < \text{lt}_{\ell,y,m,c}), \quad \text{(B.12)}$$

where $\text{lt}_{\ell,y,m,c}$ is the crop-specific threshold for cold days. Thresholds $\text{ut}_{\ell,y,m,c}$ and $\text{lt}_{\ell,y,m,c}$ are based on the 90th and 10th percentiles of temperatures (precipitation) observed during month m over the past five years. The sample of past observation is denoted as $\boldsymbol{W}_{\ell,y,d} = \{\{\mathcal{W}_{\ell,y-1,m,d}\}_{d=1}^{n_m}, \{\mathcal{W}_{c,y-2,m,d}\}_{d=1}^{n_m}, \ldots, \{\mathcal{W}_{c,y-5,m,d}\}_{d=1}^{n_m}\}$.

To set the thresholds, we rely on values traditionally used in the literature for calculating degree days. Most often, the lower threshold is set at $8°$C and the upper threshold ranges between $29°$C and $32°$C (Lobell et al., 2011; Aragón et al., 2021; Jagnani et al., 2021). We set the lower threshold at $8°$C for all crops, and the upper threshold at $30°$C for potatoes and cassava. For maize and rice, we adopt the same value used in Rising and Devineni (2020) and set the upper threshold at $29°$C.

For precipitation shocks, the thresholds are defined using the percentiles of past values only:

$$\text{ut}_{\ell,y,m,c} = P_{90}(\boldsymbol{P}_{\ell,y,d}) \quad \text{(B.13)}$$

$$\text{lt}_{\ell,y,m,c} = P_{10}(\boldsymbol{P}_{\ell,y,d}). \quad \text{(B.14)}$$

Positive values of $\mathcal{W}^{(+)}_{\ell,y,m,c}$ represent days that are hotter (or wetter) than expected, while positive values of $\mathcal{W}^{(-)}_{\ell,y,m,c}$ represent days that are colder (or drier) than expected.

Figure B.1 presents the impulse response functions (IRFs) of agricultural production for rice, maize, potato, and cassava in response to different types of weather surprises: cold, hot, dry, and wet. Each panel shows the effects over several months, with percentage changes in production relative to baseline levels, and shaded areas indicating the 68% and 95% confidence

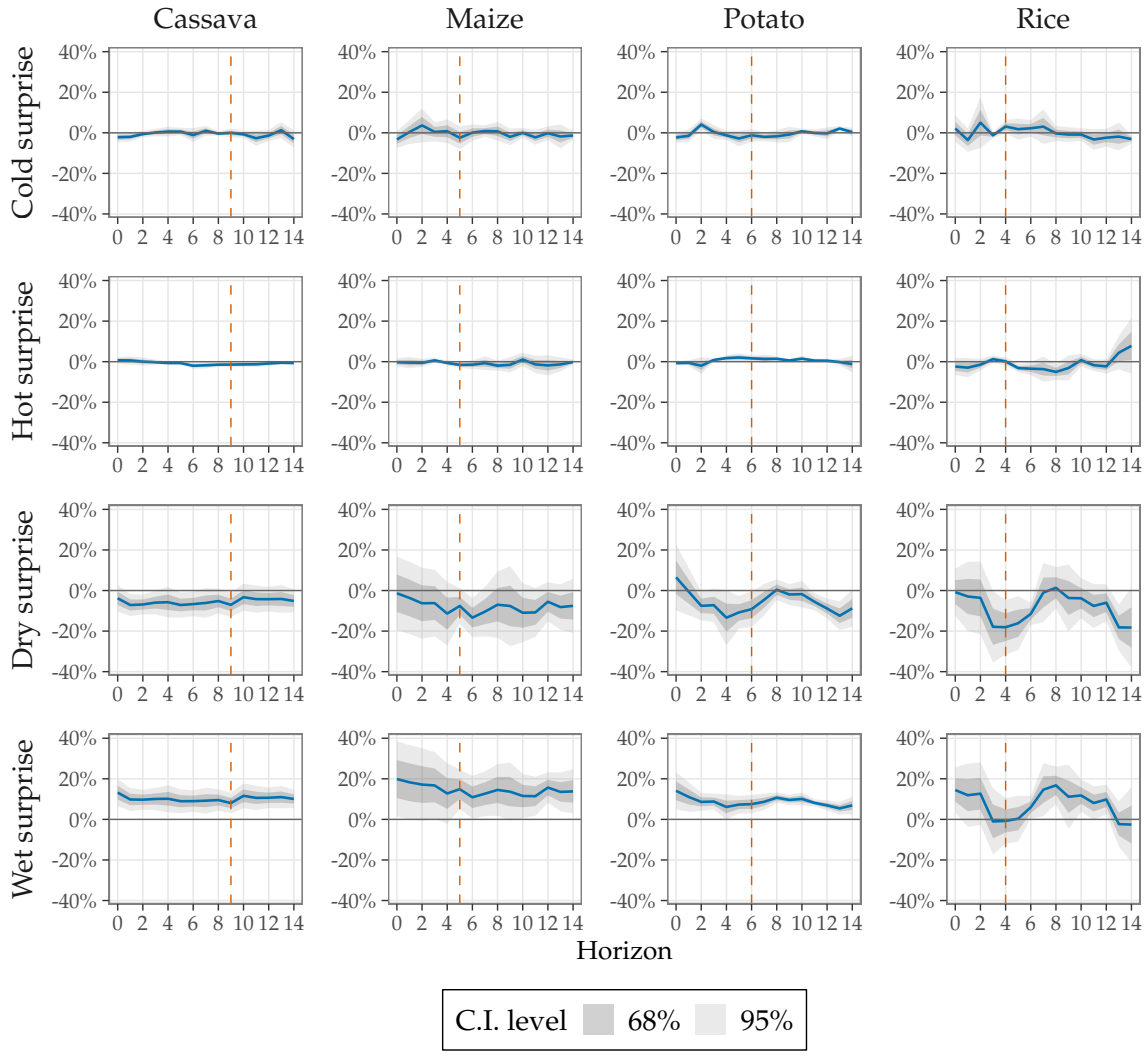

Notes: The panels show the crop-specific impulse response function of monthly agricultural production to a one standard deviation (SD) increase in the surprise weather variable, which is defined as a 1 SD increase with respect to the historical average. Horizon 0 represents the month of the shock. The shaded areas represent the 95% and 68% confidence intervals with region-level clustered standard errors. The orange dashed bars represent the average growth duration.

Figure B.1. Agricultural Production Response to Positive and Negative 1 Standard Deviation Weather Shocks.

intervals.

Cold surprises generally have mixed effects across different crops. Cold surprises imply a negative effect on impact, but this is statistically significant only at the 68% confidence level. Much of the variation in temperature effects is actually driven by hot surprises, which create substantial declines in cassava, maize, and rice. However, the magnitude of these responses is much smaller than in the previous quantitative assessment. The main reason is that these responses cannot be directly compared, as the surprise index changes the units of interpretation of the responses.

Regarding precipitation, the dry surprises reveal a stark vulnerability in certain crops. All

types of crops are heavily impacted, showing a sharp reduction of up to -20%. In contrast, wet surprises generally result in positive outcomes for agricultural production. All crops benefit from wetter conditions, showing production increases of up to 20%.

Note again that these IRFs are qualitatively quite different from the outcomes obtained in the rest of the paper. These differences emerge from the way weather shocks are measured. Our measure of weather shocks gives similar weight to all observations without recursive treatment. In contrast, Natoli (2024) proposes a recursive formulation to disentangle the standard part of the weather from its surprise component. This separation filters out a fraction of the information in weather shocks, leading to differences in the measured effects of weather shocks.

To illustrate the mechanism, consider a farmer facing extreme and consecutive weather shocks. In our case, the farmer will be equally harmed by each realization over time. However, under the surprise treatment, the impact of the second shock will be relatively less significant as the farmer will have learned from the first shock. In practice, two consecutive weather shocks should be detrimental, as a farmer has no possibility to hedge against a second shock once crops are already planted.

Appendix C Temporal Aggregation

Most studies on the effects of weather shocks on agricultural production rely on annual data. The Peruvian data allow us to conduct the analysis at a finer temporal scale, namely, monthly. In this section, we examine the measures of weather shocks according to data aggregation. Specifically, we aggregate monthly production data into quarters and years. These three levels of aggregation allow us to replicate the analysis from section 3, showing the effects of precipitation or temperature shocks using a Local Projection framework. The Impulse Response Functions in Figure C.1 show the agricultural production response to temperature shocks (top) or precipitation shocks (bottom), expressed monthly (blue), quarterly (yellow), or annually (purple). Interestingly, we observe that the shapes of the response functions are very similar when production data are aggregated monthly or quarterly for most crops and both types of shocks. However, annual aggregation produces responses that underestimate the effects of shocks on production, and in the case of precipitation for maize and potatoes, even leads to opposite conclusions. The level of data aggregation significantly affects the measured impact of weather shocks on agricultural production. Monthly and quarterly data provide a more detailed and accurate picture of these impacts compared to annual data. When access to such finer scale data is possible, monthly or quarterly data should be preferred to annual data.

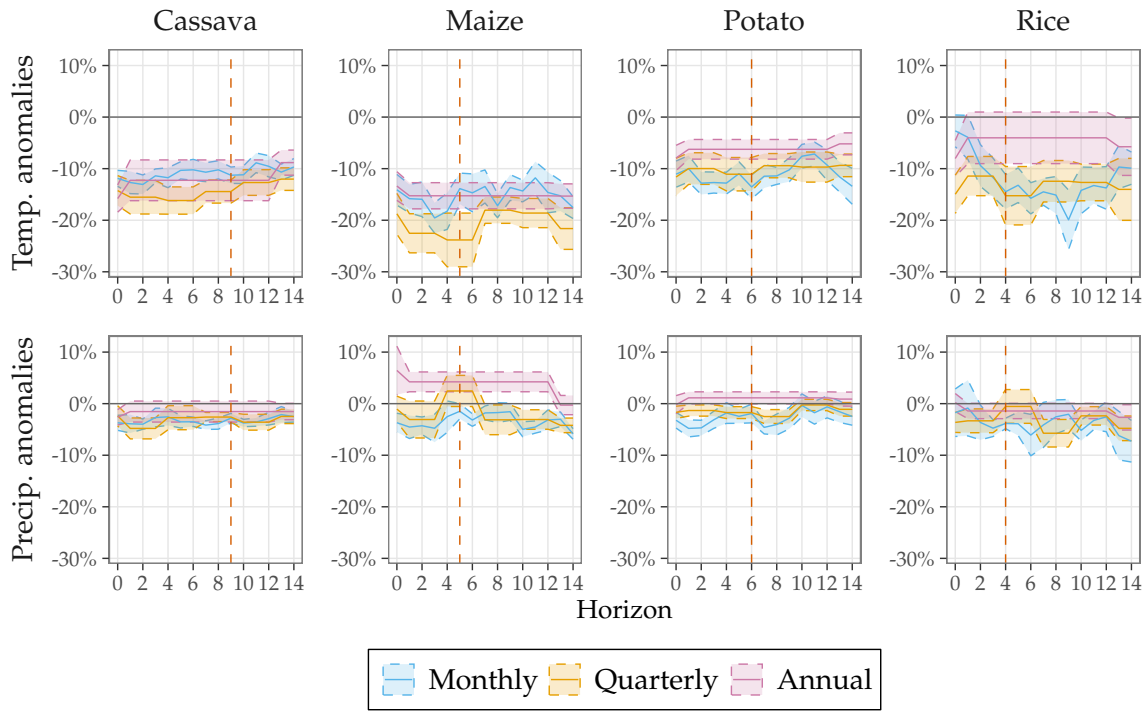

Notes: The panels show the crop-specific impulse response function of monthly/quarterly/annual agricultural production to a one standard deviation (SD) increase in the surprise weather variable, which is defined as a 1 SD increase with respect to the historical average. Horizon 0 represents the month of the shock. The colored areas represent the 68% confidence intervals with region-level clustered standard errors. The orange dashed bars represent the average growth duration.

Figure C.1. Agricultural Production Response to a Weather Shock, Using Either Monthly, Quarterly, or Annual Data.

Appendix D Vector Autoregression and Local Projections

To investigate the economic impact of weather-induced losses in the agricultural sector, we employ two approaches: a structural vector autoregression model (SVAR) and local projections (LPs). SVAR models are widely used for forecasting purposes, as they capture dynamic interdependencies across time series. In contrast, LPs offer greater flexibility by estimating impulse responses directly at each forecast horizon without imposing a rigid system structure. Both complementary methodologies allow us to assess how agricultural loss shocks propagate through the economy.

Consider the following structural form with p lags:

$$BY_t = \Gamma_0 + \sum_{l=1}^{p} \Gamma_l Y_{t-l} + \varepsilon_t, \tag{D.15}$$

where Y_t is a vector of k endogenous variables at time t, B is a $k \times k$ matrix representing contemporaneous interactions, Γ_0 contains the model intercepts, Γ_l are $k \times k$ matrices for

lagged interactions, and ε_t is a vector of white noise errors.[24]

LPs offer an alternative to traditional Vector Autoregressions (VARs), such as the model specified in Equation D.15, where the dynamic behavior of a set of variables Y_t is described by a system of autoregressive equations with lagged values and contemporaneous interactions. In a VAR, impulse response functions (IRFs) are derived from the entire estimated system, which requires strong assumptions about the structure and dynamics across all horizons. In contrast, as previously mentioned, LPs estimate the response of the outcome variable directly at each forecast horizon, typically using the following linear regression for each horizon h:

$$Y_{t+h} = A_0(h) + \sum_{l=1}^{p} \Gamma_l(h) Y_{t-l} + \varepsilon_{t+h}, \tag{D.16}$$

where Y_{t+h} is the variable of interest at horizon h, X_t represents the shock or treatment variable at time t, and the lagged terms Y_{t-l} control for past values of the outcome variable. The coefficient β_h provides the impulse response at each horizon. This method allows for more flexibility, as it estimates the IRF horizon by horizon, without relying on the entire system's structure as in VARs.

References

Acevedo, S., Mrkaic, M., Novta, N., Pugacheva, E. and Topalova, P. (2020). The effects of weather shocks on economic activity: What are the channels of impact? *Journal of Macroeconomics* 65: 103207, doi:10.1016/j.jmacro.2020.103207. 5

Aragón, F. M., Oteiza, F. and Rud, J. P. (2021). Climate change and agriculture: Subsistence farmers' response to extreme heat. *American Economic Journal: Economic Policy* 13: 1–35, doi:10.1257/pol.20190316. 23, iv

Auerbach, A. and Gorodnichenko, Y. (2011). Fiscal multipliers in recession and expansion. doi:10.3386/w17447. 14, 15, 16

Auffhammer, M., Hsiang, S. M., Schlenker, W. and Sobel, A. (2013). Using weather data and climate model output in economic analyses of climate change. *Review of Environmental Economics and Policy* 7: 181–198, doi:10.1093/reep/ret016. 7, viii

[24] To transform this model into its reduced form, Equation D.15 is premultiplied by B^{-1}: $Y_t = A_0 + \sum_{l=1}^{p} A_l Y_{t-l} + u_t$, where $A_0 = B^{-1}\Gamma_0$, $A_l = B^{-1}\Gamma_l$ for $l \in \{1, 2, \ldots, p\}$, and $u_t = B^{-1}\varepsilon_t$, *i.e.*, a linear combination of the structural shocks ε_t. The estimation of the reduced-form model allows to estimate the coefficients in A_0 and in A_l, as well as the covariance matrix Σ_u of u_t. However, to uniquely identify this model, we need to impose certain restrictions. In a system with k variables, $k \times (k-1)/2$ restrictions are necessary to separate the shocks from each other clearly. To do this, we adopt the Cholesky decomposition with short-term constraints. More specifically, we set the upper triangular elements of B to zero and normalize its diagonal elements to 1. This normalization allows the shocks' scale to be comparable, while the lower triangular elements of B can be freely estimated. More details can be found in Breitung et al. (2004).

Aybar, C., Fernández, C., Huerta, A., Lavado, W., Vega, F. and Felipe-Obando, O. (2020). Construction of a high-resolution gridded rainfall dataset for Peru from 1981 to the present day. *Hydrological Sciences Journal* 65: 770–785, doi:10.1080/02626667.2019.1649411. vii

Bareille, F. and Chakir, R. (2024). Structural identification of weather impacts on crop yields: disentangling agronomic from adaptation effects. *American Journal of Agricultural Economics* 106: 989–1019, doi:10.1111/ajae.12420. 5

Barrios, S., Bertinelli, L. and Strobl, E. (2010). Trends in rainfall and economic growth in Africa: A neglected cause of the African growth tragedy. *Review of Economics and Statistics* 92: 350–366, doi:10.1162/rest.2010.11212. 7, vii

Blakeslee, D., Fishman, R. and Srinivasan, V. (2020). Way down in the hole: Adaptation to long-term water loss in rural India. *American Economic Review* 110: 200–224, doi:10.1257/aer.20180976. 5

Blanc, E. and Schlenker, W. (2017). The use of panel models in assessments of climate impacts on agriculture. *Review of Environmental Economics and Policy* 11: 258–279, doi:10.1093/reep/rex016. 6

Breitung, J., Brüggemann, R. and Lütkepohl, H. (2004). *Structural Vector Autoregressive Modeling and Impulse Responses*. Cambridge University Press, chap. 4. 159–196, doi:10.1017/cbo9780511606885.005. 27

Buchhorn, M., Smets, B., Bertels, L., De Roo, B., Lesiv, M., Tsendbazar, N.-E., Herold, M. and Fritz, S. (2020). Copernicus global land service: Land cover 100m: collection 3: epoch 2019: Globe. *Version V3. 0.1)[Data set]* doi:10.5281/zenodo.3939050. viii, ix

Burke, M. and Emerick, K. (2016). Adaptation to climate change: Evidence from us agriculture. *American Economic Journal: Economic Policy* 8: 106–40, doi:10.1257/pol.20130025. 2, 6

Castellanos, E., Lemos, M., Astigarraga, L., Chacón, N., Cuvi, N., Huggel, C., Miranda, L., Vale, M. M., Ometto, J., Peri, P., Postigo, J., Ramajo, L., Roco, L. and Rusticucci, M. (2022). Central and south america. In Pörtner, H. O., Roberts, D. C., Tignor, M., Poloczanska, E. S., Mintenbeck, K., Alegría, A., Craig, M., Langsdorf, S., Löschke, S., Möller, V., Okem, A. and Rama, B. (eds), *Climate Change 2022: Impacts, Adaptation and Vulnerability. Contribution of Working Group II to the Sixth Assessment Report of the Intergovernmental Panel on Climate Change*. Cambridge, UK and New York, USA: Cambridge University Press, 1689–1816, doi:10.1017/9781009325844. 2

Chen, S., Chen, X. and Xu, J. (2016). Impacts of climate change on agriculture: Evidence from China. *Journal of Environmental Economics and Management* 76: 105–124, doi:10.1016/j.jeem.2015.01.005. 4

Colacito, R., Hoffmann, B. and Phan, T. (2019). Temperature and growth: A panel analysis of the United States. *Journal of Money, Credit and Banking* 51: 313–368, doi:10.1111/jmcb.12574. 3, 5

Crost, B., Duquennois, C., Felter, J. H. and Rees, D. I. (2018). Climate change, agricultural production and civil conflict: Evidence from the Philippines. *Journal of Environmental Economics and Management* 88: 379–395, doi:10.1016/j.jeem.2018.01.005. 13

Cui, X., Gafarov, B., Ghanem, D. and Kuffner, T. (2024). On model selection criteria for climate change impact studies. *Journal of Econometrics* 239: 105511, doi:10.1016/j.jeconom.2023.105511. 3

Cui, X. and Xie, W. (2022). Adapting agriculture to climate change through growing season adjustments: Evidence from corn in China. *American Journal of Agricultural Economics* 104: 249–272, doi:10.1111/ajae.12227. 14

D'Agostino, A. L. and Schlenker, W. (2016). Recent weather fluctuations and agricultural yields: implications for climate change. *Agricultural Economics* 47: 159–171, doi:10.1111/agec.12315. 2, 4, 6, 7, vii

Dell, M., Jones, B. F. and Olken, B. A. (2012). Temperature shocks and economic growth: Evidence from the last half century. *American Economic Journal: Macroeconomics* 4: 66–95, doi:10.1257/mac.4.3.66. 5, 9

Deschênes, O. and Greenstone, M. (2007). The economic impacts of climate change: Evidence from agricultural output and random fluctuations in weather. *American Economic Review* 97: 354–385, doi:10.1257/aer.97.1.354. 2, 6, 7, viii

Faccia, D., Parker, M. and Stracca, L. (2021). Feeling the heat: extreme temperatures and price stability. ECB Working Paper, doi:10.2139/ssrn.3981219. 5, 20

Gallic, E. and Vermandel, G. (2020). Weather shocks. *European Economic Review* 124: 103409, doi:10.1016/j.euroecorev.2020.103409. 18, 19, 21

Gammans, M., Mérel, P. and Ortiz-Bobea, A. (2017). Negative impacts of climate change on cereal yields: statistical evidence from France. *Environmental Research Letters* 12: 054007, doi:10.1088/1748-9326/aa6b0c. 4, 11

Hatfield, J. L. and Prueger, J. H. (2015). Temperature extremes: Effect on plant growth and development. *Weather and climate extremes* 10: 4–10, doi:10.1016/j.wace.2015.08.001. 16

Huerta, A., Aybar, C. and Lavado-Casimiro, W. (2018). PISCO temperatura v.1.1. Tech. rep., SENAMHI - DHI, Lima-Perú. vii

Jagnani, M., Barrett, C. B., Liu, Y. and You, L. (2021). Within-season producer response to warmer temperatures: Defensive investments by Kenyan farmers. *The Economic Journal* 131: 392–419, doi:10.1093/ej/ueaa063. 2, 4, 5, 23

Jordà, Ò. (2005). Estimation and inference of impulse responses by local projections. *American Economic Review* 95: 161–182, doi:10.1257/0002828053828518. 3, 10, 13

Kolstad, C. D. and Moore, F. C. (2020). Estimating the economic impacts of climate change using weather observations. *Review of Environmental Economics and Policy* 14: 1–24, doi:10.1093/reep/rez024. 6

Lesk, C., Rowhani, P. and Ramankutty, N. (2016). Influence of extreme weather disasters on global crop production. *Nature* 529: 84–87, doi:10.1038/nature16467. 6

Letta, M., Montalbano, P. and Pierre, G. (2022). Weather shocks, traders' expectations, and food prices. *American Journal of Agricultural Economics* 104: 1100–1119, doi:10.1111/ajae.12258. 14

Li, M. (2023). Adaptation to expected and unexpected weather fluctuations: Evidence from Bangladeshi smallholder farmers. *World Development* 161: 106066, doi:10.1016/j.worlddev.2022.106066. 4

Lobell, D. B., Bänziger, M., Magorokosho, C. and Vivek, B. (2011). Nonlinear heat effects on African maize as evidenced by historical yield trials. *Nature climate change* 1: 42–45, doi:10.1038/nclimate1043. 23

Massetti, E., Mendelsohn, R. and Chonabayashi, S. (2016). How well do degree days over the growing season capture the effect of climate on farmland values? *Energy Economics* 60: 144–150, doi:10.1016/j.eneco.2016.09.004. 14

Mendelsohn, R., Nordhaus, W. D. and Shaw, D. (1994). The impact of global warming on agriculture: a Ricardian analysis. *The American Economic Review* : 753–771. 6

Miao, R., Khanna, M. and Huang, H. (2016). Responsiveness of crop yield and acreage to prices and climate. *American Journal of Agricultural Economics* 98: 191–211, doi:10.1093/ajae/aav025. 4

Natoli, F. (2024). The macroeconomic effects of unexpected temperature shocks. doi:10.2139/ssrn.4160944. 18, 20, 21, 22, 25

Ortiz-Bobea, A., Ault, T. R., Carrillo, C. M., Chambers, R. G. and Lobell, D. B. (2021). Anthropogenic climate change has slowed global agricultural productivity growth. *Nature Climate Change* 11: 306–312, doi:10.1038/s41558-021-01000-1. 6

Ortiz-Bobea, A. and Just, R. E. (2012). Modeling the structure of adaptation in climate change impact assessment. *American Journal of Agricultural Economics* 95: 244–251, doi:10.1093/ajae/aas035. 4

Ortiz-Bobea, A., Wang, H., Carrillo, C. M. and Ault, T. R. (2019). Unpacking the climatic drivers of US agricultural yields. *Environmental Research Letters* 14: 064003, doi:10.1088/1748-9326/ab1e75. 4

Parry, M., Canziani, O., Palutikof, J., Linden, P. van der and Hanson, C. (2007). Fourth assessment report: Climate change 2007: The AR4 synthesis report. *Geneva: IPCC. URL http://www. ipcc. ch/ipccreports/ar4-wg1. htm* . 2, 7, vii

Powell, J. and Reinhard, S. (2016). Measuring the effects of extreme weather events on yields. *Weather and Climate Extremes* 12: 69–79, doi:10.1016/j.wace.2016.02.003. 4

Rising, J. and Devineni, N. (2020). Crop switching reduces agricultural losses from climate change in the United States by half under RCP 8.5. *Nature Communications* 11, doi:10.1038/s41467-020-18725-w. 23

Schlenker, W. and Roberts, M. J. (2009). Nonlinear temperature effects indicate severe damages to us crop yields under climate change. *Proceedings of the National Academy of sciences* 106: 15594–15598, doi:10.1073/pnas.0906865106. 6

Schmitt, J., Offermann, F., Söder, M., Frühauf, C. and Finger, R. (2022). Extreme weather events cause

significant crop yield losses at the farm level in German agriculture. *Food Policy* 112: 102359, doi:10.1016/j.foodpol.2022.102359. 4

Sesmero, J., Ricker-Gilbert, J. and Cook, A. (2018). How do African farm households respond to changes in current and past weather patterns? A structural panel data analysis from Malawi. *American Journal of Agricultural Economics* 100: 115–144, doi:10.1093/ajae/aax068. 5

Skees, J. R., Hartell, J. and Murphy, A. G. (2007). Using index-based risk transfer products to facilitate micro lending in Peru and Vietnam. *American Journal of Agricultural Economics* 89: 1255–1261, doi:10.1111/j.1467-8276.2007.01093.x. 13

Stock, J. H. and Watson, M. W. (2001). Vector autoregressions. *Journal of Economic Perspectives* 15: 101–115, doi:10.1257/jep.15.4.101. 19

Tack, J., Barkley, A. and Hendricks, N. (2017). Irrigation offsets wheat yield reductions from warming temperatures. *Environmental Research Letters* 12: 114027, doi:10.1088/1748-9326/aa8d27. 4

Taraz, V. (2018). Can farmers adapt to higher temperatures? Evidence from India. *World Development* 112: 205–219, doi:10.1016/j.worlddev.2018.08.006. 4

Welch, J. R., Vincent, J. R., Auffhammer, M., Moya, P. F., Dobermann, A. and Dawe, D. (2010). Rice yields in tropical/subtropical asia exhibit large but opposing sensitivities to minimum and maximum temperatures. *Proceedings of the National Academy of Sciences* 107: 14562–14567, doi:10.1073/pnas.1001222107. 4, 14

Yu, J. and Goh, G. (2019). Estimating non-additive within-season temperature effects on maize yields using bayesian approaches. *Scientific reports* 9: 18566, doi:10.1038/s41598-019-55037-6. 4

Online Appendix (not for Publication)

The Dynamic Effects of Weather Shocks on Agricultural Production

This online appendix includes two sections. First, Online Appendix A provides details on the data used in the article. More specifically, Online Appendix A.1 provides details on how agricultural production is specified by time, crop, and region in the analysis. Next, Online Appendix A.2 explains the temporal and spatial aggregation of daily weather data into monthly regional metrics. Online Appendix A.3 presents the macroeconomi data. Second, Online Appendix B outlines the methodology for calculating the weather-adjusted agricultural loss (WCAL) metric used in the macroeconomic analysis.

Table of Contents

Online Appendix A Data

Online Appendix A.1 Regional Agricultural Production Data

Our primary source of agricultural data is derived from monthly agricultural reports, *El Agro en Cifras*, produced by the Ministry of Agriculture and Irrigation of Peru (MINAGRI) spanning from 2001 to 2019.[25] These reports provide agroeconomic indices and agricultural production figures at both regional and national levels. We extracted data on production (measured in tons) and on the planted and harvested areas (measured in hectares) for each of the primary crops cultivated in Peru across 25 administrative regions, covering the period from January 2001 to December 2015. It is important to note that observations after 2016 are no longer reported on a monthly basis but are presented quarterly; therefore, they are excluded from our analysis. Each monthly report presents data as a cumulative sum from January to the respective reporting month. To convert the production data into net flows, we apply a first-difference filter.

[25] https://www.midagri.gob.pe/portal/boletin-estadistico-mensual-el-agro-en-cifras.

Four main crops are analyzed in this study: potato (*papa*), cassava (*yuca*), rice (*arroz cáscara*), and maize (*maíz amarillo duro*).[26] These selected crops collectively represent a substantial share of agricultural production, comprising 53% of the cultivated surface and 37% of the total production in Peru.[27] To ensure the validity of our data over the same years of observation, we cross-referenced them with the Food and Agriculture Organization data (FAOSTAT) and, observed similar quantities (see Table OA.1). According to the FAO data, the crops we focus on constitute 41% of the cultivated surface and 31% of the total quantity produced. The slight differences observed between the figures provided by the monthly reports produced by the Peruvian Ministry and those reported by the FAO are ascribed to the fact that the former focus solely on the main crops, while the latter are more exhaustive.

Table OA.1. Main Agricultural Cultures in Peru.

	FAO data		MINAGRI data	
	Total surface	Share	Total surface	Share (%)
Maize	7,349,640	16,4	4,227,147	14.7
Starchy corn			2,948,963	10.3
Rice, paddy	5,359,251	12.0	5,320,330	18.5
Coffee, green	4,999,410	11.1	-	-
Potatoes	4,213,436	9.4	4,151,734	14.5
Barley	2,253,611	5.0	2,233,429	7.8
Plantains and others	2,227,709	5.0	-	-
Wheat	2,158,122	4.8	2,102,246	7.3
Cassava	1,425,493	3.2	1,418,054	4.9
Sugar cane	1,112,131	2.5	1,032,231	3.6
Beans, dry	1,104,473	2.5	686,788	2.4

Notes: The products in bold are those studied in this study. The total surfaces correspond to the sum of national harvested surfaces, from 2001 to 2015, in hectares. Maize corresponds to Dent corn in the MINAGRI data. No distinction is made between Dent corn and Starchy corn in FAO data. Source: FAO and MINAGRI. Authors' estimate.

Agricultural production variations are both spatial and temporal. Regarding the spatial variability of agricultural production, a first overview is given in Figure OA.1. The maps show that each region's share of total production during the period is heterogeneous and specific

[26] Two types of maize are reported in the reports. We refer to *maíz amarillo duro*, or "Dent corn," as "Maize."

[27] While the Peruvian agricultural report includes data for other crop types, these exhibit numerous missing observations and do not encompass a sufficiently large time span for inclusion in the quantitative analysis.

to each crop. Regions marked with gray hatching are excluded from the analysis. These regions either lack production for certain crops or have production concentrated in a very short period of four months or less, with zero production the rest of the time, making the analysis of weather shock propagation difficult. This is the case for example, of the Puno department in southeastern Peru, for which rice production is concentrated between April and June and is zero the rest of the year. This region is therefore excluded from the analysis.[28] Nevertheless, only a few regions are excluded, and they contribute little to overall production, leading to a final sample ranging from 16 regions for rice to 23 for maize.

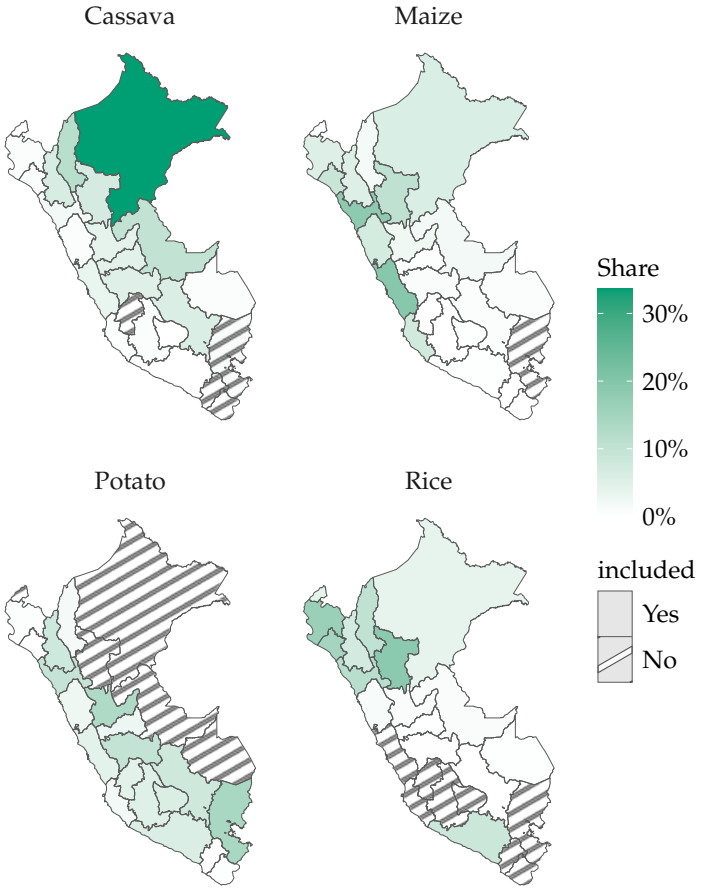

Notes: Distribution of production of each crop by administrative region. For each map, the sum of the distributions across regions equals 1. Source: MINAGRI. Author's estimate.

Figure OA.1. Regional Distribution of Crop Production by Administrative Regions.

Another way to represent the spatial heterogeneity of production is by topography. Peru is geographically diverse in terms of climate and geographical topology, typically divided into three climate areas: coastal, highlands, and Amazon rainforest. These areas exhibit very different climatic conditions due to their proximity to the sea and different altitudes. As ex-

[28] Regions with no reported agricultural production or with zero production for at least eight consecutive months are excluded from the analysis.

plained by Aragón et al. (2021), the coastal area is a narrow strip extending from the seashore to 500 meters above sea level (masl) with a semi-arid climate, warm temperatures, and little precipitation. The highlands extend from 500 masl to almost 7,000 masl, although most agriculture ceases below 4,000 masl, with a much cooler and wetter climate and seasonal precipitation in spring and early summer. Finally, the Amazon rainforest area is characterized by tropical weather with significant rainfall. A map dividing the Peruvian territory into these three natural regions is is shown in Figure OA.2. The map is based on data available on the Geo GPS Peru website.[29] Because natural regions do not always correspond to administrative regions, three variables are created for each area to represent the share of each natural region type in the administrative region.

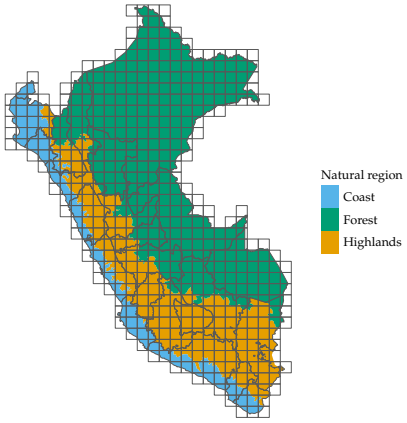

Source: Geo GPS Peru.

Figure OA.2. Natural Regions in Peru.

Regarding temporal variability, we first examine national-level crop-specific temporal patterns. The curves in Figure OA.3, representing the national monthly production of each crop over the analysis period, indicate strong seasonality in the data. Interestingly, some crops (potato and rice) exhibit a clear and regular pattern, whereas others (cassava and maize) are more volatile. A positive trend is also observed for cassava.[30]

[29] See https://www.geogpsperu.com/2019/11/mapa-de-regiones-naturales-costa-sierra.html.

[30] This positive trend is potentially due to the increase in agrarian land resulting from deforestation of the Amazon rainforest, where a large share of cassava is produced. See Figure OA.1.

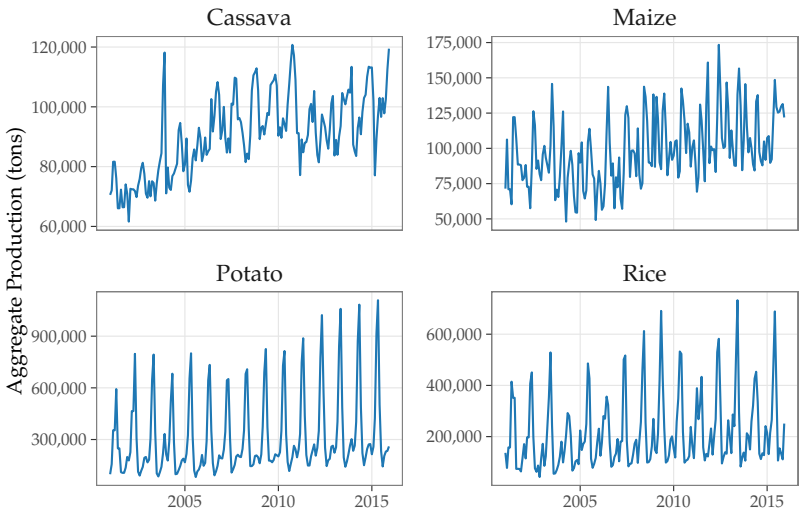

Notes: The graphs show the evolution of monthly crop production, summed over all administrative regions. For cassava, two observations (2007-06-01 and 2007-07-01) were identified as erroneous and replaced by a linear interpolation between May and July 2007. Source: MINAGRI. Author's estimate.

Figure OA.3. National Monthly Crop Production for Selected Crops (in Tons).

In Figure OA.4, we document regional differences and seasonality by averaging monthly production over different types of natural regions. Seasonal patterns are observed more closely in these graphs. For example, potato production sharply increases between March and May before decreasing. In contrast, maize displays differentiated seasonal cycles depending on the natural region. In coastal regions, there is only one production peak, in June. In forested areas, there are two main peaks: a high peak in February and a smaller peak in July. The example of cassava shows that production can be highly concentrated in one area, specifically in the forest, where more than half of the production is located. In contrast, maize production is more evenly distributed.

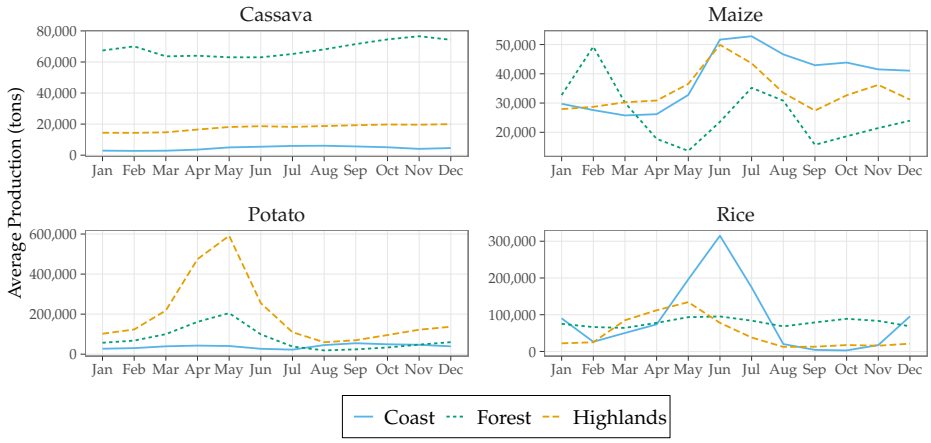

Notes: The graphs show the sum of each crop production, broken down by month and weighted by the share of the natural region. Source: MINAGRI. Author's estimate.

Figure OA.4. Crop Production by Months and Natural Regions (in Tons).

Online Appendix A.1.1 Definition of Agricultural Production

In agricultural economics, it is common to express agricultural production as yields by dividing it by the planted land surface. However, with monthly data, a significant number of observations exhibit zero values for the planted area or production, resulting in an inability to calculate yields for those months. In the article, we express agricultural production as its normalized value, where normalization consists of dividing the production value by the historical regional monthly average. Normalizing allows to correct for the size effect stemming from regional heterogeneity in production. In a nutshell, we first calculate the crop-specific average production over the entire period (January 2001 to December 2015) on a monthly basis for each region. Then, we express monthly agricultural production relative to this average. The remainder of this section explains our methodology in more details.

In a first step, we calculate the crop-specific average production over the entire period (January 2001 to December 2015) on a monthly basis for each region

$$\overline{y}_{c,i,m} = \frac{1}{n} \sum_{t=1}^{n} y^{\text{raw}}_{c,i,m,t}, \tag{OA.1}$$

where $y^{\text{raw}}_{c,i,m,t}$ represents the agricultural production reported for crop c in region i in month m at date t, and n is the number of periods with reported production values.

Then, in a second step, we express agricultural production relative to the average:

$$y_{c,i,m,t} = \begin{cases} \dfrac{y^{\text{raw}}_{c,i,m,t}}{\overline{y}_{c,i,m}}, & \overline{y}_{c,i,m} > 0 \\ 0, & \overline{y}_{c,i,m} = 0 \end{cases}. \tag{OA.2}$$

Values of $y_{c,i,m,t} > 1$ means that the production for crop c in region i during month m of year t is higher than the average monthly production for that crop and region over the period 2001 to 2015. For example, a value of 1.5 means that the production is 50% higher than average. Conversely, values of $y_{c,i,m,t} < 1$ correspond to production levels lower than the average monthly production for that crop and region over the period 2001 to 2015. For example, a value of 0.8 means that the production is 20% lower than average. Lastly, values of $y_{c,i,m,t} = 1$ indicate that the average production for that crop in that region and month over the period is equal to the average.

Online Appendix A.2 Weather and Climate Data

Our analysis uses weather anomalies and controls for ENSO events. This section presents the sources and methods used to align the data with the agricultural data at the same spatial and temporal scales.

Online Appendix A.2.1 Weather Anomalies

To construct the weather shock series, we consider daily grid temperature and precipitation data, aggregated at the monthly level for each region of Peru. We follow Barrios et al. (2010) and demean weather observations at the grid level. The means are the monthly historical values observed over the past 30 years. Next, we aggregate the values at the regional and monthly levels. The aggregation process is described in detail in this appendix. In summary, the obtained variables—temperature and precipitation anomalies—are deviations from the historical average.

Gridded weather data. We obtained temperature data from PISCOt V1.1, and precipitation data from PISCOp V2.0. These datasets provide gridded daily temperature data and precipitation, for Peru. The data were collected from January 1981 to December 2016. The grid has a 0.1° spatial resolution (10 km). The data sets are developed by the SENAMHI (the National Service of Meteorology and Hydrology of Peru). The methodology that led to the construction of this data set is explained by Huerta et al. (2018) for temperatures and by Aybar et al. (2020) for precipitation.[31]

From grid data to regional data. Agricultural production is available at the regional level. Therefore, it is necessary to map grids and regions to aggregate the weather data at the regional level. In addition, shocks such as excessive temperatures or rainfall occurring in agricultural areas should not be accounted for in the same way as shocks occurring in urban geographic land. For example, the weather conditions of a grid cell where 90% of the surface is used for agricultural production should matter more than those of a cell with 10% of the agricultural surface. When aggregating the weather data, we must identify where agricultural regions are located in Peru to give these regions more weight in the aggregation procedure. To do so, we rely on data from Copernicus, a European program for monitoring the Earth using satellite and *in situ* data managed by the European Commission.[32] We use the 2015 Peru data with a 100m resolution.

Regional weather anomalies. What are the relevant weather shocks for predicting agricultural production? Parry et al. (2007) documented a large negative sensitivity of crop production to extreme daytime weather variables. Building on this observation, we construct our temperature variable by computing the average monthly maximum temperature, and our precipitation variable is defined as the sum of the monthly rainfall. Following D'Agostino and Schlenker (2016), transformations of the weather data are first performed at the scale of the

[31] Data can be obtained from https://drive.google.com/drive/folders/1eGqhmJXBJfFSzUFz2RVqtbKIlOphpkcs for temperatures and from https://piscoprec.github.io/webPISCO/en/ for precipitation.

[32] The data are freely available: https://land.copernicus.eu/global/products/lc. The share of agricultural land for each grid cell is shown on the map in Figure OA.5.

grid cells and then aggregated at a monthly frequency for each region. Let $\mathcal{T}_{c,y,m,d}$ and $\mathcal{P}_{c,y,m,d}$ denote the temperature and precipitation observed in cell c on day $d = \{D1, D2, ...D31\}$, month $m = \{M1, M2, ...M12\}$ and year $y = \{2001, 2002, ..., 2015\}$. The temperature variable denoted $\mathcal{T}_{c,y,m}$ is defined here as the average of the most extreme meteorological events observed over the sequence of days within the considered month m in cell c, whereas the precipitation variable denoted $\mathcal{P}_{c,y,m}$ is defined as the sum of the observed daily values:

$$\mathcal{T}_{c,y,m} = \frac{1}{N_{dm}} \sum_{d=1}^{N_{dm}} \mathcal{T}_{c,y,m,d}, \quad \mathcal{P}_{c,y,m} = \sum_{d=1}^{N_{dm}} \mathcal{P}_{c,y,m,d}, \tag{OA.3}$$

where N_{dm} is the number of days within month m.

We measure the distance of the weather variable from its monthly average to assess the relative intensity of one weather shock with respect to the other realizations. Let $\mathcal{W}_{c,y,m}$ denote one of the two weather measures, temperature or precipitation, observed in cell c, month m and year y. The abnormal realization of the weather is expressed as follows:

$$W_{c,y,m} = \mathcal{W}_{c,y,m} - \overline{\mathcal{W}}_{c,\bullet,m}, \tag{OA.4}$$

where $\overline{\mathcal{W}}_{c,\bullet,m} := (y_T - y_0 + 1)^{-1} \sum_{y=y_0}^{y_T} \mathcal{W}_{c,y,m}$ denotes the average value of the weather data in cell c observed during a specific month m from year y_0 to year y_T. We set $y_0 = 1986$ and $y_T = 2015$ so that the average is computed over a period of 30 years, which is a standard practice in the literature to define climate normals (see, *e.g.*, Deschênes and Greenstone, 2007; Auffhammer et al., 2013).

Cell-specific weather anomalies are then aggregated at a monthly regional level. To accomplish this, for each region, we simply calculate the average of the anomalies from each cell, weighting each term according to two measures. The first is the proportion ω_c^{area} of the cell to the total surface area of the region. The second is the proportion $\omega_c^{\text{cropland}}$ that the cell represents in the agricultural production of the region. Refer to the map in Figure OA.5 for a representation of these shares, where the values are calculated from the Land Cover map data (Buchhorn et al., 2020).

The weather anomaly variable is defined at each date t (year y and month m) as follows:

$$W_{i,t} = \frac{\sum_{c \in \mathcal{R}_i} \omega_c^{\text{area}} \omega_c^{\text{cropland}} W_{c,t}}{\sum_{c \in \mathcal{R}_i} \omega_c^{\text{area}} \omega_c^{\text{cropland}}}, \tag{OA.5}$$

where $\mathcal{R}_i$ denotes the set of cells that fall in region i.

We apply this procedure to both temperature and precipitation observations to derive the

temperature anomaly $T_{i,t}$ and the precipitation anomaly $P_{i,t}$ in region i at time t. We interpret a large value of $T_{i,t}$ as excess heat (measured in ℃) with respect to its historical average. Similarly, we interpret a large value of $P_{i,t}$ as an excess humidity (measured in millimeters of rain) with respect to its historical average.

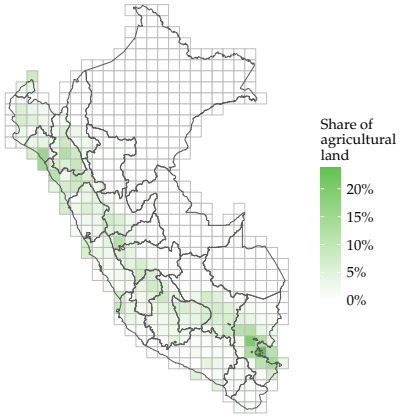

Notes: 2015 data, 100m resolution. Source: Author's estimate using data from Buchhorn et al. (2020).

Figure OA.5. Share of Agricultural Area in the Cell, for Each Cell of the Grid.

Online Appendix A.2.2 ENSO Oscillations

To explore the cause-and-effect relationship, local projections are typically built under the assumption that weather shocks (or any regressor of interest) are unexpected. However, our sample also includes El Niño and La Niña events. Notably, these climate phenomena are characterized by their predictable occurrence, diverging from the typical unexpected nature of weather shocks. Even though farmers are still surprised by the magnitude of the weather shocks during ENSO events, they can adapt by adjusting their crop mix before the weather shock materializes, introducing a potential bias in the quantitative analysis. To circumvent this issue, we use ENSO variations as a control variable to account for the expectational effect that ENSO may have on the projection. These ENSO fluctuations are classified using the Oceanic Niño Index, which computes a three-month average of the sea surface temperature anomalies in the central and eastern tropical Pacific Ocean. We collect this index from the Golden Gate Weather Service.[33] An El Niño (or La Niña) event is defined by a period of five consecutive three-month periods with an index above 0.5 (or below -0.5 for a La Niña event).

Online Appendix A.3 Macroeconomic Data

Because the data-generating process of our agricultural data is driven by alternative sources of randomness, such as economic shocks unrelated to the weather, we include macroe-

[33] See https://ggweather.com/enso/oni.htm.

conomic data as control variables. The goal of these control variables is to isolate the effect of weather variables on agricultural production from any other sources of fluctuation. By holding constant values for the control variables, any changes in the outcome can be attributed solely to the variable of interest, rather than the combined effects of multiple variables. This makes it possible to draw more accurate conclusions regarding the causal relationship between weather shocks and agricultural output. To consider these potential effects, control variables based on macroeconomic data for the Peruvian economy taken from the data warehouse of *the Banco Central de Reserva del Peru* are included.[34] The following series are included: the Peruvian Consumer Price Index (CPI), Food Price Index (FPI), Sol/US Exchange rate, national interest rate, GDP index and a sectoral index for industrial production. Note that all the control variables are national aggregates given on a monthly basis. Nominal variables (*e.g.*, exchange rate, FPI, and CPI) are detrended by calculating their growth rate. GDP and industrial production indices are expressed as percentage deviations from the Hodrick-Prescott filter to control our projections from the effects stemming from aggregate demand and supply shocks. A similar transformation is applied to the interest rate, as the latter exhibits a downward trend in the considered time span. In addition, we control for international variations that may affect the production of each culture by including their respective commodity prices using data from the International Monetary Fund.[35]

Online Appendix B Weather-Adjusted Agricultural Losses

The weather component of agricultural losses, W_t (see Equation 10 in the paper), is defined using a variable we denoted y_t^{ω} and termed "weather-adjusted agricultural production" (see, again, Equation 10 in the paper) following a five steps procedure.

Step 1. Estimating Weather Shock Contributions. In the first step, the contribution of weather shocks to a given crop (c) and time horizon (h) in each time period (t) is estimated. The weather shock contribution ($\Gamma_{c,i,t,h}$) is determined by considering the temperature ($T_{i,t}$) and precipitation ($P_{i,t}$), along with their respective coefficients ($\beta_{c,h}^T$ and $\beta_{c,h}^P$). This contribution is calculated as follows:

$$\Gamma_{c,i,t,h} = \beta_{c,h}^T T_{i,t-h} + \beta_{c,h}^P P_{i,t-h}. \tag{OA.6}$$

Step 2. Calculating Quantity Weights. In the second step, we compute the quantity weights used in the third step. For each crop and date, these weights are defined by summing the

[34] Data are taken from the Central Bank of Peru, where the Real Exchange Rate token is *PN01259PM*, Exports is *PN01461BM*, Food CPI is *PN01336PM*, CPI is *PN01270PM*, industrial GDP is *PN02079AM*, GDP *PN01773AM*, and interest rate is *PN07819NM*. All seasonal components are removed from the time series, excluding the interest rates.

[35] International commodity prices have been taken from the IMF Primary Commodity Price System website.

monthly agricultural production over regions, expressed in monetary terms. The weights are calculated as follows:

$$\omega_{c,t} = \sum_i y^{\text{raw}}_{c,t,i} \times p_c, \tag{OA.7}$$

where $y^{\text{raw}}_{c,t,i}$ represents the raw agricultural production in tons and p_c is the average selling price of crop c in our sample.

Step 3. Weather-Adjusted Agricultural Production. Moving on to the third step, we calculate the weather-adjusted agricultural production ($y^{\omega}_{c,t}$) for each crop (c) at each date (t) is computed. This is achieved by summing the significant crop-specific contributions of weather ($\Gamma_{c,i,t,h}$) to agricultural production across regions as follows:

$$y^{\omega}_{c,t} = \sum_h \sum_i \frac{\mathbb{1}_{\text{signif}_{c,i,t,h}} \times \Gamma_{c,i,t,h} \times \omega_{c,t}}{\text{card}(I_{c,t})}, \tag{OA.8}$$

where $\text{card}(I_{c,t})$ is the number of regions that produce crop c at time t, and the characteristic function $\mathbb{1}_{\text{signif}_{c,it,h}}$ equals 1 when the contribution is significantly different from 0 (based on the 95% confidence intervals of the coefficients $\beta^{T}_{c,h}$ and $\beta^{P}_{c,h}$), and 0 otherwise.

Step 4. Aggregating Crop-Specific Production. In the fourth step, crop-specific weather-adjusted agricultural production is aggregated at the national level, considering the quantity weights ($\omega_{c,t}$):

$$y^{\omega}_{t} = \frac{\sum_c y^{\omega}_{c,t}}{\sum_c \omega_{c,t}}, \tag{OA.9}$$

where $\omega_{c,t}$ are the quantity weights computed in the second step.

Step 5. Expressing Weather-Adjusted Production as a Deviation. Finally, in the fifth step, the national weather-adjusted production is expressed as a loss or deviation from its trend. The trend is obtained using a Hodrick-Prescott filter:

$$\text{WCAL}_t = -100 \times (y^{\omega}_{t} - \overline{y^{\omega}_{t}}). \tag{OA.10}$$

A negative sign is applied to ensure that the positive values of WCAL_t correspond to losses rather than gains. Intuitively, W_t measures the percentage loss of agricultural value-added from weather shocks.